

Sophie Tønneberg  
Marte Aarflot Strandheim

# Ionic Conductivity Measurements in Aqueous and Molten Salt Electrolytes

Målinger av elektrisk ledningsevne i vandige  
elektrolytter og saltsmelter

Graduate thesis in Chemical Engineering  
Supervisor: Espen Sandnes  
Co-supervisor: Geir Martin Haarberg  
May 2023



Sophie Tønneberg  
Marte Aarflot Strandheim

# **Ionic Conductivity Measurements in Aqueous and Molten Salt Electrolytes**

Målinger av elektrisk ledningsevne i vandige  
elektrolytter og saltsmelter

Graduate thesis in Chemical Engineering  
Supervisor: Espen Sandnes  
Co-supervisor: Geir Martin Haarberg  
May 2023

Norwegian University of Science and Technology  
Faculty of Natural Sciences  
Department of Materials Science and Engineering









DEPARTMENT OF  
MATERIALS SCIENCE AND ENGINEERING

TKJE3001 - BACHELOR IN CHEMICAL ENGINEERING

---

# Ionic Conductivity Measurements in Aqueous and Molten Salt Electrolytes

*Målinger av elektrisk ledningsevne i vandige elektrolytter og  
saltsmelter*

---

***Authors:***

Sophie Tønneberg  
Marte Aarflot Strandheim

***Supervisors:***

Associate Prof. Espen Sandnes  
Prof. Geir Martin Haarberg

May 2023

# Summary of Bachelor's Thesis

**Project no.** IMA-B-4-2023

**Submission Date:** 20.05.2023

**Authors:** Sophie Tønneberg and Marte Aarflot Strandheim

**Supervisors:** Espen Sandnes and Geir Martin Haarberg

**Employer:** IMA NTNU

**Contact Persons:** Sophie Tønneberg, 91242494, sophietonneberg@gmail.com  
Marte Aarflot Strandheim, 40219329, marte.strandheim@hotmail.com

**Key Words:** Aluminium, the chloride process, Alcoa smelting process,  
bipolar cell, impedance measurements, electrical conductivity

**Pages:** 59

**Attachments:** 9

**Availability:** Open



# Abstract

In a time of great focus on the green transition, the aluminium industry encounters significant obstacles concerning more climate-friendly aluminium production. Alcoa's chloride and electrolysis process is an alternative that can contribute to reaching climate goals, and is currently the only alternative method to Hall-Héroult that has reached industrial production. The process involves electrolysis of  $\text{AlCl}_3$  dissolved in a melt of alkali chlorides. Although this process has its advantages, there are still challenges associated with the electrolyte. In this thesis, the electrical conductivity of salt melts with various compositions of  $\text{NaCl}$ ,  $\text{KCl}$ ,  $\text{LiCl}$ , and  $\text{AlCl}_3$  was investigated using impedance measurements. A U-shaped test cell was developed from Pyrex, which was first tested by impedance measurements in aqueous salt solutions. The test cell was then optimised and produced in quartz for high-temperature experiments with salt melts.

The results show that the U-shaped cell design provides impedance measurements with high accuracy and precision. Quartz was chosen as the material for the cell used in high-temperature experiments, as quartz has a very low thermal expansion coefficient. Repeated use of corrosive chloride salts in the quartz cell led to visible damage, and eventually the cell fractured during experimental work. If there is a need for the test cell to be utilised in several experiments, an alternative material to quartz should be considered.

The conductivity obtained from experimental measurements agreed well with tabular values in both aqueous salt solutions and salt melts. The results from high-temperature experiments showed that factors such as cation size, complex formation, and melt composition had a significant impact on electrical conductivity. In general, it was observed that increasing levels of  $\text{NaCl}$  and  $\text{LiCl}$  increased the conductivity, while  $\text{KCl}$  and  $\text{AlCl}_3$  decreased conductivity. The increase in temperature resulted in a nearly linear increase in conductivity. In an industrial context, a compromise between salts with high and low conductivity would be necessary, as  $\text{AlCl}_3$  is a crucial component, and  $\text{LiCl}$  is an expensive option. The liquidus of salt mixtures should also be considered, as different compositions have different liquidus.



# Sammendrag

I en tid med stort fokus på det grønne skiftet, står aluminiumsindustrien overfor en sentral utfordring knyttet til mer klimavennlig aluminiumsproduksjon. Alcoas klorid- og elektrolyseprosess er et alternativ som kan bidra til å nå klimamålene, og er i dag den eneste alternative metoden til Hall-Héroult som har nådd industriell produksjon. Prosessen innebærer elektrolyse av  $\text{AlCl}_3$  løst i smelte av alkaliklorider. Selv om denne prosessen har sine fordeler, er det fortsatt utfordringer knyttet til elektrolytten. I denne oppgaven undersøkes den elektriske ledningsevnen til saltsmelter med ulike sammensetninger av  $\text{NaCl}$ ,  $\text{KCl}$ ,  $\text{LiCl}$  og  $\text{AlCl}_3$  ved hjelp av impedansmålinger. Det ble utviklet en U-formet testcelle av Pyrex som først ble testet ved impedansmålinger i vandige saltløsninger. Deretter ble testcellen optimalisert og produsert i kvarts for høytemperatursforsøk med saltsmelte.

Resultatene viser at det U-formede celledesignet gir impedansmålinger med høy nøyaktighet og presisjon. Kvarts ble valgt som materiale for cellen brukt i høytemperatursforsøk, da kvarts har en svært lav termisk ekspansjonskoeffisient. Gjennatt bruk av korrosive kloridsalter i kvartscellen førte til synlig slitasje, før cellen knuste under eksperimentelt arbeid. Dersom det er nødvendig at testcellen skal kunne benyttes i flere forsøk, bør et annet materiale enn kvarts vurderes.

Konduktivitet funnet fra eksperimentelle målinger stemte godt overens med tabulære verdier i både vandige saltløsninger og saltsmelter. Resultatene fra høytemperatursforsøkene viste at faktorer som kationstørrelse, kompleksdannelse og smeltekomposisjon hadde betydelig innvirkning på den elektriske ledningsevnen. Generelt ble det observert at et økende innhold  $\text{NaCl}$  og  $\text{LiCl}$  økte konduktiviteten, mens  $\text{KCl}$  og  $\text{AlCl}_3$  senket konduktiviteten. Konduktiviteten økte tilnærmet lineært med økende temperatur. I industriell sammenheng vil et kompromiss mellom salter med høy og lav ledningsevne være nødvendig, da  $\text{AlCl}_3$  er en avgjørende komponent i aluminiumsproduksjonen og  $\text{LiCl}$  er en kostbar løsning. Smeltepunktene til saltblandingene bør også tas i betraktning, ettersom ulike komposisjoner gir ulike smeltepunkt.



# Preface

You are about to read "Ionic Conductivity Measurements in Aqueous and Molten Salt Electrolytes". This bachelor's thesis is written at NTNU, Department of Materials Science and Engineering, during spring 2023.

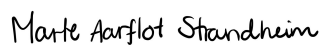
Several factors influenced our choice of this topic for our bachelor's thesis. We were drawn to the opportunity to contribute to pioneering research while conducting relevant laboratory experiments. Additionally, our previous assignments and lectures on electrochemistry and material science made it a subject of particular interest.

This thesis fulfills the requirements for the completion of a bachelor's degree in chemical engineering at The Norwegian University of Science and Technology (NTNU). From January to May 2023, we dedicated ourselves to the research and writing process. Our supervisors, Espen Sandnes and Geir Martin Haarberg, collaborated with us to formulate the research question, and despite encountering challenges, our perseverance led to valuable insights and results.

We hereby declare that this work has been carried out independently and according to the examination regulations of The Norwegian University of Science and Technology (NTNU).



Sophie Tønneberg



Marte Aarflot Strandheim

Trondheim, May 2023





# Acknowledgements

- Associate Prof. Espen Sandnes<sup>1</sup> for your commitment in spending late evenings and numerous hours on proofreading, providing guidance, and offering words of support.
- Prof. Geir Martin Haarberg<sup>1</sup> for always being available for questions and thoroughly reviewing the assignment countless times. Your close supervision of the laboratory work and writing has been highly appreciated.
- Senior Engineer Marthe Folstad<sup>1</sup> and Senior Engineer Anita Storsve<sup>1</sup> for guidance in the laboratory, always willing to help.
- Senior Engineer Astrid Salvesen<sup>1</sup> and Staff Engineer Sebastian Bete<sup>1</sup> for making a new customised quartz cell on short notice.
- Senior Research Scientist Karen Sende Osen<sup>2</sup> and SINTEF for granting us the opportunity to borrow the laboratory, equipment, and the gold furnace.
- Our dearest colloquium group for endless support and the countless memorable moments we have shared over the course of three years.
- Department of Materials Science and Engineering, IMA, NTNU, for their financial support in our work.

<sup>1</sup> Norwegian University of Science and Technology (NTNU), Trondheim.

<sup>2</sup> SINTEF Industri, Trondheim.



# Table of Contents

Summary	i
Abstract	iii
Sammendrag	v
Preface	vii
Acknowledgements	ix
Table of Contents	xi
List of Figures	xv
List of Tables	xviii
<b>1 Introduction</b>	<b>1</b>
<b>2 Theory</b>	<b>3</b>
2.1 Electrolyte resistance and conductivity . . . . .	3
2.1.1 Electrical and physical properties . . . . .	3
2.1.2 Electrochemical conductivity measurements . . . . .	4
2.2 Aqueous salt electrolytes . . . . .	4
2.2.1 Electrical conducting salt solutions . . . . .	4
2.2.2 Ion size and conductivity . . . . .	5
2.2.3 Concentration dependence . . . . .	6
2.2.4 Temperature dependence of electrical conductivity . . . . .	6
2.2.5 Activation energy of electrical conductivity in aqueous solutions	7
2.3 Molten salt electrolytes . . . . .	7
2.3.1 Properties of molten salts . . . . .	7
2.3.2 Electrical conductivity in molten salt . . . . .	8
2.3.3 AlCl <sub>3</sub> properties . . . . .	9
2.3.4 Activation energy of electrical conductivity in molten salts . .	10
2.4 Bipolar cell for the production of aluminium . . . . .	11
2.4.1 Cell structure . . . . .	11
2.4.2 The chloride smelting process . . . . .	12
2.5 Factors influencing electrolysis efficiency . . . . .	13

2.5.1	Electrolyte composition . . . . .	13
2.5.2	Complex ions . . . . .	14
2.5.3	Electrode material . . . . .	14
2.5.4	Temperature . . . . .	14
2.5.5	Interpolar distance . . . . .	15
2.5.6	Energy consumption in aluminium electrolysis . . . . .	16
2.6	Impedance measurements . . . . .	17
2.6.1	Impedance . . . . .	17
2.6.2	Electrochemical impedance spectroscopy (EIS) . . . . .	18
2.6.3	Nyquist plot . . . . .	19
<b>3</b>	<b>Experimental</b>	<b>20</b>
3.1	Materials and equipment . . . . .	20
3.2	Aqueous solutions . . . . .	21
3.2.1	Pyrex cell design . . . . .	21
3.2.2	Impedance measurements at room temperature . . . . .	22
3.2.3	Impedance measurements at varying temperatures . . . . .	23
3.3	Molten salt . . . . .	24
3.3.1	Quartz cell design . . . . .	24
3.3.2	Impedance measurements with molten NaCl and KCl . . . . .	25
3.3.3	Impedance measurements of melts with hygroscopic compounds . . . . .	26
<b>4</b>	<b>Results and Discussion</b>	<b>28</b>
4.1	Aqueous solutions . . . . .	28
4.1.1	Cell design . . . . .	28
4.1.2	Measurements at room temperature . . . . .	28
4.1.3	Measurements at varying temperature . . . . .	32
4.2	Molten salts . . . . .	34
4.2.1	Cell design . . . . .	34
4.2.2	Eutectic composition of NaCl-KCl . . . . .	36
4.2.3	80-20 mol% NaCl-KCl . . . . .	38
4.2.4	Eutectic composition of NaCl-KCl + 20 mol% LiCl . . . . .	39
4.2.5	Eutectic composition of NaCl-KCl + 3 mol% AlCl <sub>3</sub> . . . . .	40
4.2.6	Eutectic composition of NaCl-KCl + 3 mol% AlCl <sub>3</sub> + 1 g LiCl . . . . .	44
4.2.7	Comparison of conductivity and activation energy for all molten salt compositions . . . . .	45
4.3	Sources of Error . . . . .	47
4.3.1	Uncertainties for the conductivity measurements in aqueous solutions . . . . .	47

4.3.2	Uncertainties for the conductivity measurements in molten salts . . . . .	48
<b>5</b>	<b>Conclusion</b>	<b>49</b>
<b>6</b>	<b>Further Work</b>	<b>51</b>
	<b>References</b>	<b>53</b>
	<b>Appendices</b>	<b>60</b>
<b>A</b>	<b>Varying concentrations in aqueous solutions</b>	<b>62</b>
<b>B</b>	<b>Cell constant quartz cell</b>	<b>64</b>
<b>C</b>	<b>Calculation of salt compositions in high temperature experiments</b>	<b>66</b>
<b>D</b>	<b>Weighed quantity of salt for experiments with hygroscopic molten salts</b>	<b>67</b>
<b>E</b>	<b>Finding average measured resistance from Nyquist plots</b>	<b>68</b>
<b>F</b>	<b>Calculations of standard and percentage deviations</b>	<b>70</b>
<b>G</b>	<b>Impedance measurements at varying temperatures for aqueous solutions</b>	<b>71</b>
<b>H</b>	<b>All measurements molten salts</b>	<b>73</b>
<b>I</b>	<b>HSE data</b>	<b>75</b>



# List of Figures

2.1	Solvation of $\text{Na}^+$ with water [16]. . . . .	5
2.2	Conductivity of LiCl, NaCl and KCl as a function of temperature [34].	9
2.3	Phase diagram of NaCl and $\text{AlCl}_3$ [37]. . . . .	10
2.4	Alcoa's bipolar cell [41]. . . . .	11
2.5	Voltage and energy comparison for the Alcoa Smelting Process (ASP) and Hall-Hérout single cell equivalent [41]. . . . .	12
2.6	Phase diagram NaCl-KCl [46]. . . . .	15
2.7	The impedance Z plotted as a planar vector using polar coordinates [53]. . . . .	18
2.8	Nyquist plot for a Randels circuit [56]. . . . .	19
3.1	Dimensions and the final Pyrex cell. . . . .	21
3.2	Gamry Reference 620 Potentiostat. . . . .	22
3.3	Experimental equipment for impedance measurements in aqueous solutions. . . . .	22
3.4	Experimental setup in water bath for varying the temperature. . . .	23
3.5	Dimensions and final product. . . . .	24
3.6	The setup of the customised cell inside the quartz crucible. The electrodes are covered in salt. . . . .	25
3.7	The figures provide a total overview of the experimental setup for the gold furnace. . . . .	26
3.8	Crushed $\text{NaAlCl}_4$ blended with NaCl and KCl in the quartz cell. . .	27
4.1	Nyquist plot of KCl (1 M) at 25 °C. . . . .	28
4.2	Conductivity of various NaCl concentrations at 25 °C. . . . .	30
4.3	Conductivity $[\frac{S}{cm}]$ for NaCl (1 M) and KCl (1 M) plotted against temperature [°C]. . . . .	32
4.4	Arrhenius plot for NaCl (1 M) and KCl (1 M) in aqueous solutions.	33
4.5	The quartz cell containing molten NaCl-KCl with eutectic composition inside the furnace. . . . .	34
4.6	Cell damages. . . . .	35
4.7	The conductivity of molten NaCl-KCl with eutectic composition plotted as a function of temperature. . . . .	37
4.8	The conductivity of 80-20 mol% NaCl-KCl plotted as a function of temperature. . . . .	39



4.9	The conductivity of the eutectic composition of NaCl-KCl added 20 mol% NaCl-KCl-LiCl plotted as a function of temperature. . . . .	40
4.10	Evidence of contamination seen in the quartz cell after the first experiment with AlCl <sub>3</sub> . . . . .	41
4.11	White coating seen inside the top of the crucible after the experiment.	42
4.12	The product obtained after melting 50-50 mol% NaCl-AlCl <sub>3</sub> to a homogeneous mixture at 170 °C. . . . .	42
4.13	The conductivity of eutectic NaCl-KCl composition with 3 mol% AlCl <sub>3</sub> added plotted as a function of temperature. . . . .	43
4.14	The conductivity of eutectic NaCl-KCl added 3 mol% AlCl <sub>3</sub> and 1 g of LiCl plotted as a function of temperature. . . . .	45
4.15	Comparison of all conductivity measurements of molten salt mixtures as a function of temperature. . . . .	45
4.16	Arrhenius plot for all molten salt mixtures. . . . .	46
E.1	Experimental results for impedance measurements of 80-20 mol% KCl-NaCl presented in both Nyquist plot and table, first measurement.	68
E.2	Experimental results for impedance measurements of 80-20 mol% KCl-NaCl presented in both Nyquist plot and table, second measurement.	69
E.3	Experimental results for impedance measurements of 80-20 mol% KCl-NaCl presented in both Nyquist plot and table, third measurement.	69
I.1	H/P phrases for AlCl <sub>3</sub> . . . . .	75
I.2	H/P phrases for LiCl. . . . .	75

# List of Tables

3.1	Materials and equipment used in all experimental work. . . . .	20
4.1	Resistance measurements for salt solutions of NaCl and KCl with varying concentrations. . . . .	29
4.2	Resistance measurements and tabular conductivity for salt solutions of NaCl and KCl with varying concentrations. . . . .	29
4.3	Comparison of tabular and calculated conductivity, in addition to conductivity calculated from various mixing ratios. . . . .	31
4.4	Resistance measurements and associated conductivity for eutectic NaCl-KCl composition at varying temperatures. . . . .	37
4.5	Average measured resistance and associated conductivity values for a solution containing 80 mol% NaCl and 20 mol% KCl at varying temperatures. . . . .	38
4.6	Average measured resistance and associated conductivity values for a solution containing eutectic composition of NaCl-KCl added 20 mol% LiCl at varying temperatures. . . . .	39
4.7	Average measured resistance and associated conductivity values for eutectic NaCl-KCl added 3 mol% AlCl <sub>3</sub> . . . . .	43
4.8	Average measured resistance and associated conductivity values for eutectic NaCl-KCl added 3 mol% AlCl <sub>3</sub> and 1 g LiCl. . . . .	44
4.9	The activation energies for the various molten salt composition. . . . .	46
A.1	Resistance [ $\Omega$ ] for various salt solutions. . . . .	62
A.2	Resistance [ $\Omega$ ] measurements for various mixing ratios of salt solutions. . . . .	62
A.3	Calculated cell constant for various salt solutions. . . . .	63
B.1	Resistance [ $\Omega$ ] measurements for various salt solutions in quartz cell 1. . . . .	64
B.2	Calculated cell constant for various salt solutions measured in quartz cell 1. . . . .	64
B.3	Resistance [ $\Omega$ ] measurements for various salt solutions in quartz cell 2. . . . .	65
B.4	Calculated cell constant calculations for various salt solutions measured in quartz cell 2. . . . .	65
D.1	Total mass weighed out for the mixture with eutectic composition of NaCl-KCl + 3 mol% of AlCl <sub>3</sub> . . . . .	67
D.2	Mass from the eutectic composition of NaCl-AlCl <sub>3</sub> . . . . .	67

G.1	Measurement data for NaCl at different temperatures. . . . .	71
G.2	Measurement data for KCl at different temperatures. . . . .	71
G.3	Resistance measurements, calculated conductivity and tabular conductivity for KCl (1 M) at 30 °C, 40 °C and 50 °C. . . . .	71
G.4	Resistance measurements and calculated conductivity for NaCl (1 M) at 30 °C, 40 °C and 50 °C. . . . .	72
H.1	Measurement data for eutectic composition of NaCl-KCl at different temperatures. . . . .	73
H.2	Measurement data for 80-20 mol% NaCl-KCl at different temperatures. . . . .	73
H.3	Measurement data for eutectic NaCl-KCl composition added 20 mol% LiCl at different temperatures. . . . .	73
H.4	Measurement data for eutectic NaCl-KCl composition added 3 mol% AlCl <sub>3</sub> at different temperatures. . . . .	74
H.5	Measurement data for eutectic NaCl-KCl composition added 3 mol% AlCl <sub>3</sub> and 1 g LiCl at different temperatures. . . . .	74

# 1 Introduction

The production of aluminium has been an on-going industry since the late 1800's. Charles Martin Hall and Paul Héroult invented the electrolytic reduction with carbon in 1886 known as the Hall-Héroult process. This is the only industrial production method of aluminium used until today [1]. Nevertheless, the Hall-Héroult process has its disadvantages such as poor energy efficiency and high emissions of environmental pollutants [2].

The Hall-Héroult process produces primary aluminium from alumina by electrical reduction. The alumina is extracted from bauxite using the Bayer-process. In Hall-Héroult cells, a horizontal anode surface is immersed in the cryolite electrolyte, while a single surface cathode is located at the bottom [2]. During electrolysis, the carbon anodes react with oxygen in the alumina to produce carbon dioxide and carbon monoxide, causing them to be consumed and having to be replaced every four weeks. The Hall-Héroult process is therefore faced with challenges due to its high emission of greenhouse gases and generation of waste [3].

One of the main disadvantages in producing aluminium is the high energy consumption. The Hall-Héroult process has a relatively low energy efficiency and is therefore highly demanding on electrical energy resources, resulting in high production costs [4]. The energy used in the Hall-Héroult process globally today is mainly based of fossil fuels, such as coal and nature gas. This is caused by the limited availability on renewable energy sources. In 2020, approximately 55% of the power consumption in aluminium production used coal as the main energy source [5].

The aluminium industry is confronted with a major difficulty, as the global demand for aluminium is projected to increase 2-3 times by the year of 2050 [3]. However, the industry must also reduce its total greenhouse gas emissions by half by the same year. This requires that the emissions per ton of produced aluminium must be lowered by at least 75% [3]. Developing innovative solutions is urgent for the aluminium industry to reach the mentioned goals.

Alternative processes are being explored as potential substitutes for the Hall-Héroult process to decrease energy consumption and reduce greenhouse gas emissions. Some of the processes being considered include the use of inert anodes, carbothermic reduction of alumina, and the chloride process [1]. However, only the chloride process has been implemented at an industrial scale as the "Alcoa Smelting Process"

---

(ASP). The ASP was developed in the 1970s, and involves electrolysis of  $\text{AlCl}_3$  (5-10 wt%) dissolved in alkali chlorides. Some of the main advantages of the ASP is the low working temperature ( $700^\circ\text{C}$ ), elimination of a consumable anode and less area required for the same amount of metal produced [6].

The presence of solid oxide particulates in the melts was detected by Alcoa, and found to drastically decrease the conductivity in the electrolyte. Also, aluminium ions in the melt will form complex ions with chloride, contributing to the decrease of electrical conductivity. To minimise the effect of complex formation, additional salts such as  $\text{NaCl}$  and  $\text{LiCl}$  is added in the electrolyte.  $\text{Li}^+$ -ions have a great polarisation strength which will weaken the bonds in the  $\text{AlCl}_4^-$  complex [7]. Considering the mentioned challenges, it would be relevant to look into different electrolyte compositions of molten chloride salts and their electrical conductivity.

This thesis aims to study the behaviour of relevant salts in the ASP electrolyte and designing an appropriate experimental setup. The conductivity of molten salts with various compositions of  $\text{NaCl}$ ,  $\text{KCl}$ ,  $\text{LiCl}$  and  $\text{AlCl}_3$  will be determined from impedance measurements at several temperatures.  $\text{NaCl}$  and  $\text{KCl}$  will be chosen as the primary components in the melt due to their affordability and availability of relevant data for comparison. Especially the eutectic mixture of  $\text{NaCl}$  and  $\text{KCl}$  is of interest in high temperature measurements because of its low melting point, which facilitates the experimental work. Prior to the high temperature experiments with molten salts, impedance measurements of aqueous salt solutions will be done in order to test and optimise the chosen experimental setup. A customised test cell will then be designed for the molten salt experiments.

## 2 Theory

### 2.1 Electrolyte resistance and conductivity

#### 2.1.1 Electrical and physical properties

The electrical properties of an electrolyte is determined by its ability to conduct charged particles. This is a physical property expressed as conductance ( $G$ ), and is given by the SI unit Siemens ( $S$ ). Conductance is the opposite of resistance ( $R$ ), which is a measure of opposition to current flow measured in Ohm [ $\Omega$ ] [8].

Mathematically, conductance equals to the reciprocal of resistance as shown in Equation 2.1:

$$G = \frac{1}{R} \quad (2.1)$$

Conductance is an extrinsic property, meaning that it is dependent on amount, physical size and geometry. The related intrinsic property is conductivity. Electrical conductivity ( $\kappa$ ), also known as specific conductance, refers to the degree of ease with which a solution allows the passage of electric charge. This is a physical quantity, and is defined as the inverse value of the substance's resistivity ( $\rho$ ). Resistivity refers to the electrical resistance of a conductor with a unit cross-sectional area and unit length and is a distinctive property. High resistivity indicates low conductivity, meaning that the solution is a poor conductor of electricity [9]. Resistivity and conductivity are given in Equation 2.2 and 2.3, respectively:

$$\rho = R \frac{A}{L} \quad (2.2)$$

$$\kappa = \frac{1}{\rho} \quad (2.3)$$

Equation 2.2 and 2.3 are used to derive an equation relating resistance and conductivity as shown in 2.4.

$$\kappa = \frac{1}{R} \frac{L}{A} \quad (2.4)$$

In Equation 2.4,  $\frac{L}{A}$  refers to the cell constant ( $K$ ). The cell constant is defined as the ratio of the distance between the electrodes in a conductivity cell to the cross-sectional area of the cell, as shown in equation (2.5).

---

$$K = \frac{L}{A} \quad (2.5)$$

In most cases, the cross-sectional area ( $A$ ) of the cell cannot be determined by the geometry due to non-ideal current distribution. Instead, the cell constant will have to be calculated using Equation 2.4.

### 2.1.2 Electrochemical conductivity measurements

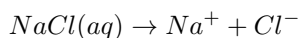
Electrical conductivity in solutions can be found by measuring the solution's resistance using a potentiostat. A potentiostat is an instrument used in electrochemistry to control the potential difference between two or more electrodes in a solution, while measuring the resulting current. To measure the resistance of a solution with a potentiostat, the instrument is set up in a two-electrode configuration, where the electrodes are placed at a known distance from each other. In a given electrolytic solution, conductivity tends to increase with decreasing distance between two electrodes. A small AC voltage is applied across the electrodes, and the resulting current is measured using the potentiostat [10].

Resistance measurements can be used to determine the cell constant experimentally by measuring the resistance of a standard solution with a known conductivity, calculating the cell constant from Equation 2.4. Once the cell constant is known, the electrical conductivity of an unknown solution can be calculated in the same conductivity cell by measuring the cell's resistance and applying the calculated cell constant.

## 2.2 Aqueous salt electrolytes

### 2.2.1 Electrical conducting salt solutions

Salts are a group of chemical compounds with a distinct electrolytic dissociation. Electrolytic dissociation involves using a solvent to divide a substance into ions. As a result, the solution's physical properties are altered, including its electrical conductivity [11]. Many salts are soluble in water, including NaCl. When NaCl dissolves in water, it dissociates into ions:



Movement of charged particles is crucial to achieve current flow and thereby electrical conductivity, and the conductivity of an electrolyte is determined by the ion mobility [12]. Ion mobility is defined as the average speed of ions per unit electric field and

---

is impacted by the ion concentration and the temperature of the electrolyte. The total ion mobility is a result of an external field force and ion movement resistance. This resistance is a result of different forces, including those between the ions and the solvent, and those within the solvent itself [13].

The solvent will influence the degree of dissociation the salt experiences, and thus influences whether the compound acts as a strong or weak electrolyte [11]. Especially the use of water as a solvent will influence the dissociation of a compound, as this is related to the significant dipole moment of water molecules. The dipole moment will cause water molecules to surround charged ions in a solution, affecting the electrostatic attraction between the ions [14]. An ion encircled by water molecules is referred to as hydrated. When moving, the ion will have to drag its hydration shell along with itself, affecting the ion's mobility [15].

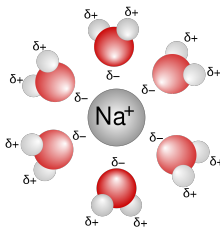


**Figure 2.1:** Solvation of  $\text{Na}^+$  with water [16].

## 2.2.2 Ion size and conductivity

The conductivity of a salt solution is dependent on the size of the ions from the dissolved salt. There are two mechanisms caused by ion size effects that will influence the conductivity; hydrodynamic resistance and electrostatic attraction between counter-ions. The hydrodynamic resistance causes a reduction in conductivity with increasing ion size, as this resistance is a function of the interfacial area between the ion and solvent. Hence, the larger ions have more interfacial area and thus a greater hydrodynamic resistance, which decreases the conductivity. However, the smaller ions will encounter greater electrostatic attraction between counter-ions, increasing the probability of ion-pairs formation. The attractive forces are greater between smaller ions because they can approach each other at less of a distance than bigger ions. As a result, ion-pairs are formed, decreasing the amount of free ions and thus the electrical conductivity [17].

$\text{NaCl}$  and  $\text{KCl}$  are extensively studied salts that are frequently reported in the scientific literature. Despite both being alkali salts with chloride as the anion



---

and equally charged cations, their cationic radii differ.  $Na^+$  has a smaller atomic radius than  $K^+$ , which results in the hydration shell of a  $Na^+$ -ion being more clearly defined compared to that of a  $K^+$ -ion. This makes the hydrated  $Na^+$ -ion larger and less mobile.  $K^+$ , on the other hand, does not have a defined solvation structure, making the hydrated radius close to the original ionic radius [18], [19].

### 2.2.3 Concentration dependence

Both NaCl and KCl dissociates completely in water and are therefore considered strong electrolytes. The solution's conductivity increases linearly with the concentration of these alkali chloride salts [20]. However, the ability of electrolyte solutions to carry current will always peak at a certain concentration for aqueous solutions. This is due to the decrease of ionic mobility associated with the concentration-enhanced electrostatic interactions between the ions in the electrolyte [21].

Electrostatic forces are determined by Coulomb's law, which states that the force of attraction varies inversely with the square of the distance between two opposite charges. The electrostatic force of attraction will therefore be powerful when the charges are adjacent, but will decline rapidly as distance between the charges increases [22]. Coulomb interactions will be more present between the ions in solutions with higher ionic concentrations than in a more dilute solution, making the prediction of conductivity in concentrated electrolytes more complex. For low ionic concentrations, their conductivity can be successfully predicted by the Debye-Hückel-Onsager theory [23], but there is no well-established theory appropriate for higher ionic concentrations. The Debye-Hückel-Onsager theory will predict a lower conductivity for more concentrated electrolytes because of its assumption of strong interionic interactions and their ability to reduce the conductivity [24].

When mixing aqueous electrolyte solutions consisting of different cations and anions, the obtained solution will experience a change in conductivity [25]. Predicting the exact change, however, is complex when there is more than a single cation-anion pair. Therefore, there is still a need for a model that successfully can predict the conductivity of multi-component systems [26].

### 2.2.4 Temperature dependence of electrical conductivity

The conductivity of an electrolyte with a higher concentration is often modelled as a function of both concentration and temperature. Firstly, the temperature of the solution will influence the degree of ion dissociation. Higher temperatures will increase the dissociation, increasing the number of free ions. Secondly, an increase in temperature will lead to a decrease in intermolecular forces, causing a rise in the

---

rate of ion migration [13]. It is also observed that the effects on temperature of the viscosity of the water and the ion mobility in aqueous solutions are relatively similar since lower viscosity implies higher conductivity [15].

### 2.2.5 Activation energy of electrical conductivity in aqueous solutions

Electrical conductivity in an aqueous electrolyte solution is dependent on its activation energy,  $E_a$ . In the temperature range of 20 - 80°C,  $E_a$  decreases nearly linearly to the temperature increase [27]. The decrease in  $E_a$  is caused by the thermal destruction of order in liquid water, indicating that  $E_a$  is a sensitive measure of the degree of order in liquid water at a given temperature [28].  $E_a$  of an aqueous electrolyte can be obtained from conductivity measurements over a certain temperature range. The correlation between conductivity and  $E_a$  is shown in Equation 2.6:

$$\kappa = \kappa_0 \exp \frac{-E_a(\kappa)}{RT} \quad (2.6)$$

where  $R$  represents the gas constant. To find  $E_a$  in an electrolyte solution, the natural logarithm of the conductivity can be plotted as a function of the inverse temperature in an Arrhenius plot. From here,  $E_a$  is found by multiplying the slope of the graph with the gas constant. Rewriting Equation 2.6 gives the function for  $\ln(\kappa)$ :

$$\ln(\kappa) = \ln(\kappa_0) - \frac{E_a(\kappa)}{RT} \quad (2.7)$$

which can be used to calculate  $E_a$ . As seen from Equation 2.7, higher  $E_a$  corresponds to lower conductivity.

## 2.3 Molten salt electrolytes

### 2.3.1 Properties of molten salts

Molten salts at high temperatures play a crucial role in various industrial applications, including metal production. Physical properties, such as density, electrical conductivity and viscosity, are critical and important to study, especially when used as electrolytes. Molten salts are composed of ions that are held together by coulombic interactions, and the ionicity of the salt is determined by the strength of these forces between the constituent ionic species. If the coulombic force is too strong, it can prevent the formation of stable ionic molten salts, leaving the salt non-ionic.

---

Therefore, the phenomenon of complex formation must be considered when studying the properties of molten salts [29].

Molten salts consist of ions with different valencies that come into direct contact with one another because there are no solvents, such as water, present. The cohesive force of the liquid arises from the coulombic attractive force between the cation and anion, which depends on their valence and radius. The cohesive force causes molecules of the same substance to be attracted to one another, and a stronger attractive force results from a higher valence and smaller radius. Smaller molecules have electrons closer to the nuclei, which limits the space for electrons to distribute. Alkali halides such as LiCl and NaCl are typically used in molten salt systems, due to their strong ionicity [30], [29].

### **2.3.2 Electrical conductivity in molten salt**

Electrical conductivity in molten salt refers to the ability of the molten salt to conduct electricity due to the presence of free charged ions. In a molten salt, the strong ionic bonds between the ions are broken due to the high temperature, and the ions become free to move, allowing them to conduct electricity [31]. Typically, a molten salt electrolyte exhibits 10-50 times higher conductivity than aqueous salt electrolytes [32]. The electrical conductivity of molten salt depends on various factors such as the type of ions present, their concentration, and the temperature of the salt. A greater conductivity can be achieved through increased ionic electrical mobility, which is correlated to temperature. The velocity of the ions increases as the temperature of the melt increases, which again will increase the conductivity of the melt. In certain cases, there may be a maximum conductivity observed at a specific temperature. This is because as the temperature rises, the melt expands, causing the counter-ions to come closer together, which will limit the conductivity [31].

Ionic bond strength affects ion mobility and conductivity. NaCl has stronger ionic bonds due to smaller  $\text{Na}^+$ -ions, resulting in a higher melting point than KCl. Although the stronger ionic bonds in NaCl restricts ion movement and conductivity, its smaller cation radius results in higher ion mobility and conductivity compared to KCl, as shown in Figure 2.2. The cations are usually the main charge carriers, thereby determining properties such as electrical conductance. The conductivity of molten salt mixtures can be affected by the presence of different cations despite having the same anion. In the case of adding  $\text{Li}^+$  to a chloride melt, the mobility of  $\text{Li}^+$ -ions is higher, resulting in an increase in conductivity [33].

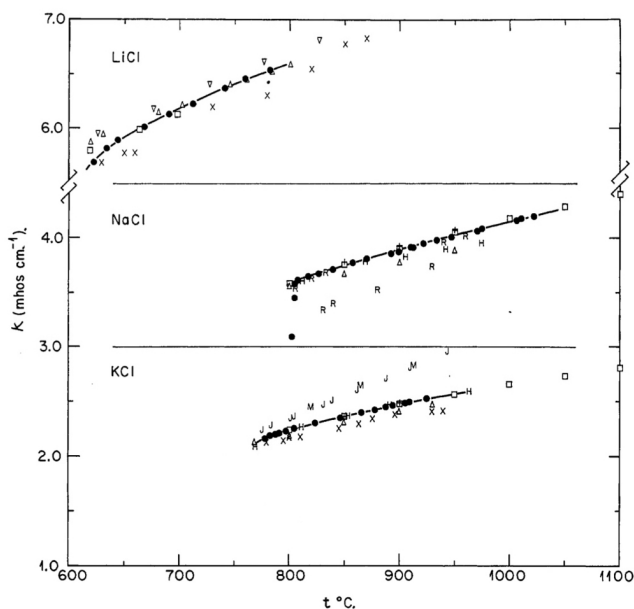


**Figure 2.2:** Conductivity of LiCl, NaCl and KCl as a function of temperature [34].

### 2.3.3 $\text{AlCl}_3$ properties

The attractive coulombic force in molten salts can occasionally be strong enough to prevent the formation of ionic melts. For example, some multivalent salts, such as  $\text{AlCl}_3$ , form melts with low melting temperatures and low ionic conductivity. This is because the strong attractive force between  $\text{Al}_3^+$  and  $\text{Cl}^-$  forms a semi-permanent bond. This completes the ionic bond inside the molecule of  $\text{Al}_2\text{Cl}_6$ , which behaves like a non-ionic molecule. Therefore, moderately weak coulombic forces are required to form molten salts.  $\text{AlCl}_3$  is a volatile salt which sublimates at  $180^{\circ}\text{C}$  and 1 atm, and can therefore not create a melt on its own [35]. However,  $\text{AlCl}_3$  forms ionic melt by adding a  $\text{Cl}^-$  donor salt such as NaCl and LiCl [36]. This can be observed in Figure 2.3.

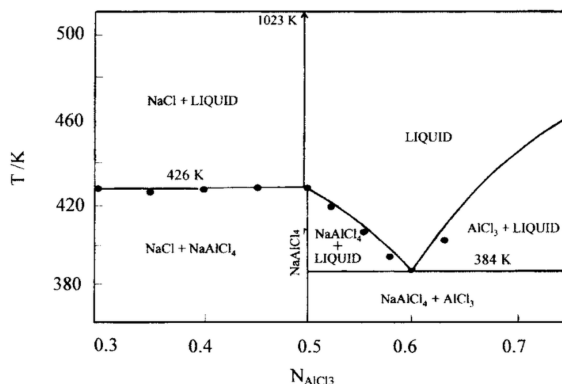


**Figure 2.3:** Phase diagram of NaCl and AlCl<sub>3</sub> [37].

The activity of AlCl<sub>3</sub> is enhanced as one moves from melts based on NaCl to melts based on LiCl. This is because the addition of Li<sup>+</sup> ions to the melt, which have a greater polarising strength than Na<sup>+</sup>-ions, weakens the bonds in the [AlCl<sub>4</sub>]<sup>-</sup> and [AlCl<sub>7</sub>]<sup>-</sup> complex grouping. This results in an increase in the activity of AlCl<sub>3</sub>. The bonds between Na<sup>+</sup>- and Li<sup>+</sup>-ions and Cl<sup>-</sup>-ions are strengthened, leading to a corresponding weakening of the [AlCl<sub>4</sub>]<sup>-</sup> and [AlCl<sub>7</sub>]<sup>-</sup> complex grouping [38].

When AlCl<sub>3</sub> is exposed to air, it readily reacts with the moisture present in the air forming HCl and Al<sub>2</sub>O<sub>3</sub>. The reaction occurs because AlCl<sub>3</sub> is a highly hygroscopic compound, meaning that it has a strong affinity for water. When exposed to air, AlCl<sub>3</sub> absorbs water vapour from the atmosphere, which reacts to form HCl and Al(OH)<sub>3</sub>. As a result, AlCl<sub>3</sub> becomes a difficult salt to handle. The reaction between AlCl<sub>3</sub> and water can be represented by the following equation:



### 2.3.4 Activation energy of electrical conductivity in molten salts

In molten salts, the activation energy of conductivity is related to ionic migration. Like aqueous salt solutions,  $E_a$  can be found from plotting the natural logarithm of conductivity as a function of the inverse temperature as shown in Equation 2.7. However,  $E_a$  of a molten salt system increases significantly if the crystallisation temperature is approached. This is due to the existence of a greater degree of order in the melt close to the melting point, inhibiting the ionic migration [39]. Nevertheless, for nearly all molten salt electrolytes, Arrhenius plots of  $\ln \kappa$  versus  $\frac{1}{T}$  are essentially linear for certain temperature ranges [40].

Lower activation energy is generally associated with higher ionic mobility and better conductivity in molten salts, as it indicates the ease with which ions can move through the liquid phase. There is a distinct increase of activation energy  $E_a$  for alkali chlorides with decreasing ratio of anion to cation radius,  $(\frac{r_a}{r_c})$ . This implies that alkali chlorides with smaller cation radii, such as LiCl and NaCl, have less activation energy of electrical conductivity and are generally better conductors [39].

## 2.4 Bipolar cell for the production of aluminium

### 2.4.1 Cell structure

The Alcoa Smelting Process (ASP) cell has a different design than the Hall-Héroult process. It is a so called multipolar design, because of its additional bipolar electrodes between the anode and cathode. These act like both anode and cathode, and are called bipolars. The high energy efficiency is gained by having multiple bipolars in a cell. The cell consists of a steel mantle which is lined with refractory materials that are thermally insulating and non-conducting, providing resistance to the corrosive chloride electrolyte. [38]

The bipolar design has some advantages over the typical Hall-Héroult cell designs, which will be discussed.

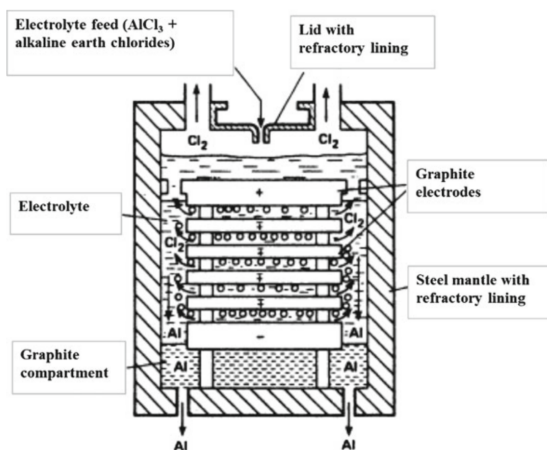


Figure 2.4: Alcoa's bipolar cell [41].

---

## 2.4.2 The chloride smelting process

The primary advantages of the aluminium chloride smelting includes:

1. Lower working temperature of 700°C, as opposed to the Hall-Héroult cell at 980°C.
2. The critical current density for the anode effect being relatively high allows for the application of higher current densities, resulting in significantly increased throughputs per cell. As a result, capital costs can be reduced.
3. Elimination of the need for a consumable carbon anode, which accounts for more than 7 % of the total cost in Hall-Héroult's process.
4. The bipolar chloride cell offers near theoretical power efficiencies, leading to direct savings in energy costs.
5. The chloride cells can withstand power interruptions better than the Hall-Héroult cells, as they generate less excess heat and have a much lower temperature liquid range for the electrolyte.
6. Superior metal purity is achieved with chloride electrolysis, greatly reducing undesirable contamination of sodium found in Hall-Héroult metal.

Compared to the Hall-Héroult cell's voltage of about 4.5 V, the inter-electrode cell voltage for chloride electrolysis is significantly lower, approximately 3 V. This is due to lower polarisation and electronic voltage drops. As a result, chloride electrolysis consumes at least 30 % less energy when using bipolar cells [38].

Parameter	Hall - Heroult cell	ALCOA Bipolar cell (Estimated)
Decomposition voltage	1.18 V	1.85 V
Electrode polarisation	0.50 V	0.40 V
Ionic resistance drop (electrolyte)	1.60 V	0.55 V
Electronic (electrode) resistance	1.02 V	0.02 V
<b>Total cell voltage</b>	<b>4.30 V</b>	<b>2.90 V</b>
Current efficiency	90 %	90 %
Energy efficiency	45 %	60 %
DC kWh / kg	14.2	9.6

**Figure 2.5:** Voltage and energy comparison for the Alcoa Smelting Process (ASP) and Hall-Héroult single cell equivalent [41].

The comparisons of the two processes are illustrated in Table 2.5. In theory, the bipolar cell appears to be a more sustainable option as it consumes less energy.

---

## 2.5 Factors influencing electrolysis efficiency

The efficiency of the electrolysis processes can be enhanced by high conductance electrolytes, which lower the electrical resistance of the solution. This leads to reduced production costs and increased profits. The presence of  $\text{AlCl}_3$  in molten salt reduces its ionic conductivity and increases its viscosity simultaneously. This is caused by the formation of a complex structure in the molten salt, and increases the polymerisation degree of the local structure in the molten salt. The electrical conductivity decreases as the viscosity increases.

### 2.5.1 Electrolyte composition

The two alternative compositions typically used in the Alcoa smelting process are listed below, where the second option is preferred [42]:

- 5 wt%  $\text{AlCl}_3$  + 53 wt%  $\text{NaCl}$  + 40 wt%  $\text{LiCl}$  + 0.5 wt%  $\text{MgCl}_2$  + 0.5 wt%  $\text{KCl}$  + 1 wt%  $\text{CaCl}_2$
- $5 \pm 2$  wt%  $\text{AlCl}_3$  + 53 wt%  $\text{NaCl}$  + 42 wt%  $\text{LiCl}$

The use of lithium chloride in the electrolytic bath is expensive, and the electric current efficiency in an  $\text{AlCl}_3$ - $\text{LiCl}$ - $\text{NaCl}$  system is limited to a maximum of 85 %, making it desirable to develop a more industrially advantageous composition. Through research on the electrolytic bath composition, it has been discovered that electrolysing  $\text{AlCl}_3$  with an electrolytic bath containing small amounts of  $\text{CaCl}_2$  or  $\text{MgCl}_2$ , in addition to  $\text{LiCl}$  in the  $\text{AlCl}_3$ - $\text{NaCl}$  system, resulted in high current efficiency for aluminium production [43].

The composition of the bath has been found to be critical. Presence of oxides more than 0.03 % in the bath adversely affects the conditions of the graphite electrode. Also, an increase in the amount of  $\text{AlCl}_3$  in the molten substance enhances chlorine solubility and reduces current efficiency [38].

If the  $\text{AlCl}_3$  concentration in the electrolytic bath exceeds 15 wt%, the electric conductivity decreases significantly, and the vapour pressure of the bath increases to the point where the cell voltage rises and cell operation becomes unstable. Therefore, it is preferable to keep the  $\text{AlCl}_3$  concentration below 15 wt%. If the concentration is less than 2 wt%, it is too low, and the electric power is likely to be consumed locally for purposes other than aluminium production [43].



---

### 2.5.2 Complex ions

The formation of complex groupings with  $\text{AlCl}_3$  in the chloride process for aluminium production has a significant effect on the conductivity of the electrolyte. The complex anions, such as  $[\text{AlCl}_4]^-$  and  $[\text{Al}_2\text{Cl}_7]^-$ , are larger in size than individual  $\text{Cl}^-$  ions and have lower mobility. This results in a decrease in the overall conductivity of the electrolyte, which can lead to higher energy consumption and lower efficiency in the aluminium production process. However, the formation of these complex anions is necessary to stabilise the  $\text{Al}^{3+}$ -ions and prevent the formation of  $\text{Al}_2\text{O}_3$ , which would clog the electrolytic cell. Therefore, it is important to find a balance between the formation of complex anions and maintaining an adequate conductivity for efficient aluminium production [41], [43], [44].

### 2.5.3 Electrode material

The electrode material used in the chloride process for the production of aluminium is typically graphite. Graphite is preferred due to its high electrical conductivity, low reactivity with the electrolyte, and resistance to corrosion. The use of graphite electrodes also reduces the risk of contamination from the electrode material. Additionally, the graphite electrodes can be easily shaped to meet the required dimensions for the electrolytic cell. In the chloride process, the graphite electrodes used for the anode will in principle not be consumed [43].

### 2.5.4 Temperature

Temperature is an important factor in aluminium electrolysis as it affects the solubility, conductivity and current efficiency. Maintaining a constant temperature is important for efficient and effective aluminium production. To ensure consistent operation and control, it is always better to conduct electrolysis above the melting point of aluminium, which is at  $660^\circ\text{C}$  [38]. The aluminium chloride process has definite advantages in that it can be operated at a temperature of about  $700^\circ\text{C}$ , which is about  $300^\circ\text{C}$  lower than in the Hall-Héroult process [43].

When selecting an electrolyte for electrolysis, knowledge of the eutectic composition is valuable as it indicates the electrolyte's minimum melting point. A eutectic composition is a specific composition of a mixture of two or more substances where the melting point of the mixture is at its lowest possible temperature. By employing the eutectic composition, the electrolyte can be maintained in a liquid state at a lower temperature, consequently decreasing energy consumption and improving process efficiency. Eutectic compositions usually exhibit greater stability compared to other compositions, minimising the risk of decomposition or

---

undesirable reactions throughout the electrolysis [45].

For the NaCl-KCl system, the eutectic composition occurs at a temperature of 657°C and a composition of approximately 50-50 mol% NaCl and KCl, as shown in Figure 2.6. At this temperature and composition, the NaCl-KCl mixture will form a eutectic mixture, resulting in a homogeneous liquid that has the lowest melting point of any possible mixture of the two components. This means that if the temperature of the system is lowered below the eutectic point, the mixture will solidify into a single-phase solid that has the same composition as the eutectic liquid [45].

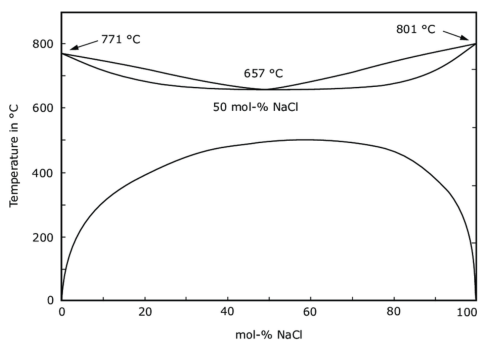


**Figure 2.6:** Phase diagram NaCl-KCl [46].

The NaCl-KCl-LiCl system is a ternary system, and the addition of LiCl will affect the eutectic temperature and the systems characteristics. The eutectic point of the NaCl-KCl-LiCl system occurs at a temperature of approximately 354°C and a composition of approximately 42 % NaCl, 32 % KCl, and 26 % LiCl [47].

### 2.5.5 Interpolar distance

To increase current efficiency, it is desirable to have a relatively small distance between the electrodes (typically 10-25 mm). The main advantage of the smaller interpolar distance is to reduce the ohmic voltage drop [38]. It has been discovered that inclining the electrodes can cause the produced aluminium to flow more easily and be removed from between the electrodes [43]. The reduced distance between the anode and cathode is evidently the primary advantage of ASP, compensating for the higher reversible decomposition voltage and slightly lower conductivity of the chloride melt [48].

---

## 2.5.6 Energy consumption in aluminium electrolysis

The minimum voltage required for an electrolysis process to occur ideally is known as the reversible voltage ( $E_{rev}$ ). However, due to electrode polarisation, there always exists a potential difference between practical and ideal situations when an electric current passes through an electrochemical cell. The degree of electrode polarisation is defined as overpotential, denoted by  $\eta_t$  and calculated as:

$$\eta_t = E - E_{rev} \quad (2.8)$$

Here,  $E$  is the applied potential, and  $E_{rev}$  is the reversible voltage or decomposition voltage. It is common to differentiate between cathodic overpotential ( $\eta_c$ ) and anodic overpotential ( $\eta_a$ ) [49].

In industry, the total cell voltage  $U$  is measured, which includes the ohmic voltage drop  $IR$  through the electrolyte and electrodes. The total cell voltage  $U$  is always considered a positive quantity and is given by:

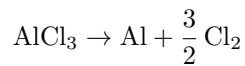
$$U = |E_{rev}| + IR + |\eta_t| \quad (2.9)$$

Here,  $I$  is the applied current,  $R$  is the resistance of the electrolyte, and  $\eta_t$  is the sum of the anode and cathode voltage, or total overpotential. Electrode reactions contribute to the cell voltage, as the cell voltage is the measured voltage difference between the two electrodes. As the current density ( $A/cm^2$ ) increases, it can cause problems such as excessive heat generation and increased wear of electrodes and cell lining. Reducing the current density too much will on the other side decrease the process efficiency, resulting in a lower current density. This can cause a decrease in aluminium production per unit time [50]. Therefore, finding the optimal current input for aluminium production is a balancing act between maximising current density to increase production rates while avoiding excessive heat generation and unwanted byproducts [2].

The Gibbs free energy equation expresses the relationship between free energy ( $\Delta G$ ), enthalpy ( $\Delta H$ ), and entropy ( $\Delta S$ ) and is given by:

$$\Delta G^0 = \Delta H^0 - T\Delta S^0 \quad (2.10)$$

The reaction for the electrolysis of  $AlCl_3$  is:



When ( $\Delta G^0$ ) is positive, the reaction or process is non-spontaneous and will only

---

occur with the input of external energy, as for electrolysis processes. The entropy change ( $\Delta S^0$ ) is usually positive because gases have more entropy than solids due to their greater freedom of motion. This indicates that  $\Delta H^0$  is the determining factor and must be greater than  $\Delta G^0$ .

## 2.6 Impedance measurements

### 2.6.1 Impedance

Impedance is a measure of the ability of a circuit to resist the flow of electrical current, and is not limited by pure ohmic resistances. The relationship between resistance, voltage and current are limited to an ideal resistor, meaning only one circuit element. An ideal resistor follows Ohm's law at all current and voltage levels, is independent of frequency and the alternating current (AC) and voltage signals through the resistor are in phase. However, in reality there will be circuit elements that display more complex behaviour as inductive or capacitive effects at nearly all frequencies [51]. Impedance is used as a more comprehensive circuit parameter to compensate for the simplifying limitations [10]. Like resistance, impedance is also measured in ohm, but the parameter is frequency-dependent. The impedance represents the relation between the current and the voltage in an AC circuit given from a modified Ohms law as shown in Equation 2.11:

$$Z(jw) = \frac{U(w)}{I(w)} \quad (2.11)$$

where  $Z$ ,  $U$  and  $I$  represent impedance, voltage and current respectively, while  $w$  and  $j$  represent the radial frequency and an imaginary component [51]. Impedance is given by the complex number  $Z = a + jb$ . Here,  $a$ ,  $b$  and  $j$  represent respectively the real part of the impedance, the imaginary part and the imaginary number. The radial frequency ( $w$ ) used in Equation 2.11 is correlated to frequency ( $f$ ) as shown in Equation 2.12 (6):

$$w = 2\pi f \quad (2.12)$$

Impedance is a vector quantity consisting of its real and imaginary contributions, and it may be plotted in a plane with rectangular or polar coordinates as shown in Figure 2.7. The real part of the impedance is found when the phase angle,  $\theta$ , equals to zero. When  $\theta$  equals to zero the impedance will be frequency-independent, but this is normally not the case [52].

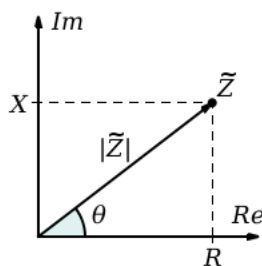


**Figure 2.7:** The impedance  $Z$  plotted as a planar vector using polar coordinates [53].

### 2.6.2 Electrochemical impedance spectroscopy (EIS)

Electrochemical impedance spectroscopy (EIS) can be used as an analytical method to investigate ionic conductivity of electrolytes, and is one of the most important electrochemical techniques [54]. In EIS, the impedance in a circuit is measured in ohms with the help of a potentiostat and a frequency analyser. The potentiostat is able to operate in a wide range of applied frequencies, from less than 1 mHz to beyond 1 MHz [55].

EIS can be used to study diffusion processes or charge- and mass transfer, and is thus able to examine specific processes that might have an influence on conductance, capacitance or resistance of an electrochemical system. EIS measures impedance by applying an alternating voltage to the circuit [55].

Practically, the electrochemical impedance is measured by applying an alternating voltage signal to the working electrode in an electrochemical cell and then measure the resulting current wave. From the applied signal and the measured wave, both the imaginary and real parts of the impedance can be extracted. Since the impedance is frequency dependent, a wide range of frequencies is applied. Varying frequencies are applied to study the resistance caused by different components in the electrochemical cell, such as solution resistance ( $R_s$ ), charge transfer resistance ( $R_{ct}$ ) and the Warburg impedance,  $W$ . The solution resistance is independent of the frequency as it is a pure ohmic resistance, while the Warburg impedance is dependent on frequency and is caused by the additional resistance generated from diffusion of species at the electrode surface. At higher frequencies, the diffusing species in an electrolyte solution do not have to move far, resulting in a smaller Warburg impedance. The diffusion force is greater at lower frequencies, and by that the Warburg impedance also increases [55]. Charge transfer resistance is the opposition to electron transfer at the electrode surface. Warburg impedance and charge transfer resistance will not be studied further as solution resistance is the

quantity of interest in salt electrolytes [51].

### 2.6.3 Nyquist plot

The final data from EIS measurements is often presented in a Nyquist plot. A Nyquist plot is formed by plotting the real part of the impedance,  $Z_{real}$ , on the X-axis and the imaginary part,  $Z_{imag}$ , on the Y-axis. In this plot, each of the points is an impedance value measured at a given frequency. The real impedance increases with decreasing frequencies [55]. Figure 2.8 shows the Nyquist plot of a Randles circuit.

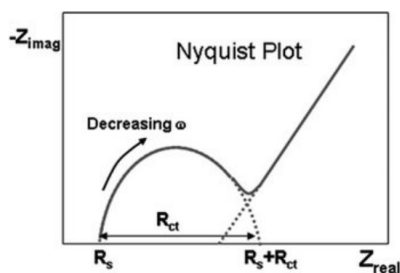


**Figure 2.8:** Nyquist plot for a Randles circuit [56].

In a Nyquist plot, the real part of the impedance is described by Equation 2.13:

$$Z = R_s + \frac{R_{ct}}{1 + w^2 + R_{ct}^2 C_{dl}^2} \quad (2.13)$$

Here,  $C_{dl}$  represents the electric double layer capacitance present at the electrode surface [51].  $C_{dl}$  refers to the charge separation at mentioned electrodes [57]. However, when determining the conductivity of salt electrolytes,  $R_s$  is the characteristic of interest.  $R_s$  is frequency-independent and can be found at the higher frequencies in a Nyquist plot. Here, at a certain frequency, the plot will intersect the real axis at the value of  $R_s$  [51].

# 3 Experimental

The following chapter provides a detailed account of the experimental procedures conducted throughout this thesis. The objective of this study was to measure the resistance and investigate the conductivity trends of various molten salt compositions. To validate the experimental setup, the resistance of aqueous salt solutions was measured in a customised Pyrex test cell. The test cell was later optimised for high temperature measurements and made in quartz.

## 3.1 Materials and equipment

The materials and equipment presented in Table 3.1 were used in the experiments.

**Table 3.1:** Materials and equipment used in all experimental work.

	<b>Materials</b>	<b>Equipment</b>
<b>Aqueous electrolytes</b>	<ul style="list-style-type: none"><li>• NaCl (VWR, CAS-number: 7647-14-4)</li><li>• KCl (VWR, CAS-number: 7447-40-7)</li></ul>	<ul style="list-style-type: none"><li>• Gamry Reference 620 Potentiostat</li><li>• Customised Pyrex test cell</li><li>• Platinum electrodes</li><li>• Laboratory water bath</li></ul>
<b>Molten salt electrolytes</b>	<ul style="list-style-type: none"><li>• NaCl (VWR, CAS-number: 7647-14-4)</li><li>• KCl (VWR, CAS-number: 7447-40-7)</li><li>• LiCl (99 %, Sigma Aldrich, CAS-number: 7447-41-8)</li><li>• AlCl<sub>3</sub> (98+ %, ThermoScientific, CAS-number: 7446-70-0)</li><li>• Argon gas</li></ul>	<ul style="list-style-type: none"><li>• Gamry Reference 620 Potentiostat</li><li>• Customised quartz test cell</li><li>• Platinum electrodes</li><li>• Gold-plated furnace</li><li>• Type S Thermocouple</li><li>• Quartz crucible with complementary lid</li><li>• Glove box</li><li>• Drying cabinet</li></ul>

---

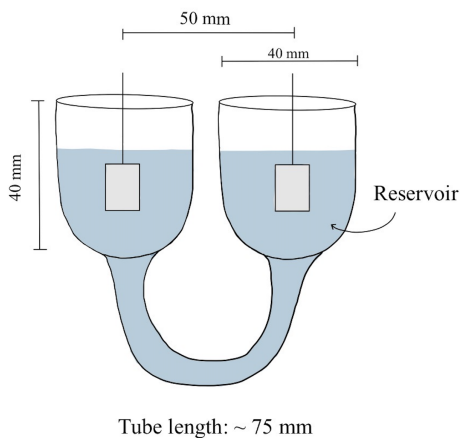
## 3.2 Aqueous solutions

### 3.2.1 Pyrex cell design

A Pyrex cell was customised for the experiments in aqueous solutions. The cell was designed as a U-shaped conductivity cell as shown in Figure 3.1b. Dimensions of the cell are presented in Figure 3.1a .

The cell was designed as a U-shaped cell to ensure high resistance values in the impedance measurements. The optimal length and diameter of the U-tube were determined by estimating the resistance of known electrolytes. Higher resistances were desired, but size limitations regarding high temperature experiments later on were also considered. This was done to create as similar experimental conditions as possible when designing the high temperature cell. The diameter of the gold furnace used in high temperature measurements put certain restrictions on the cell design, especially the diameter of the reservoirs.

The Pyrex cell was designed in a way that would make the resistance in the tube dominant compared to the resistance in the reservoir. The dimensions of the cell and the final product is shown in Figure 3.1.



(a) Dimensions of the cell.



(b) The prefabricated cell.

**Figure 3.1:** Dimensions and the final Pyrex cell.



---

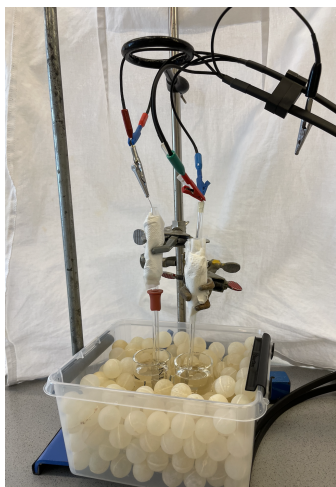
### 3.2.2 Impedance measurements at room temperature

A Gamry Reference 620 Potentiostat, as shown in Figure 3.2, was used for impedance measurements of various salt solutions of NaCl and KCl. The salt solutions measured had concentrations between 1 molar (M) and saturation. In addition, solutions with varying mixing ratios of NaCl and KCl with a total salt concentration of 1 M were measured. The potentiostat measured the samples' impedance within a frequency range of 1 MHz to 1 Hz, and the measurements were performed with the platinum electrodes completely covered by the salt solution. All the solutions were measured three times where the electrodes were removed and inserted back into place between each measurement. This was done to avoid systematic errors and obtain the variations related to electrode positioning.



**Figure 3.2:** Gamry Reference 620 Potentiostat.

The glass cell was put in a plastic container with small plastic spheres for support. The electrodes were held up by a stand with adjustable clamps, as shown in Figure 3.3a, and the electrodes used are shown in Figure 3.3b.



**(a)** Setup for aqueous solutions at room temperature.



**(b)** Platinum electrodes.

**Figure 3.3:** Experimental equipment for impedance measurements in aqueous solutions.

---

### 3.2.3 Impedance measurements at varying temperatures

The impedance measurements of KCl (1 M) and NaCl (1 M) at varying temperatures were conducted using the same potentiostat. The impedance of both solutions was measured at 30 °C, 40 °C and 50 °C in a laboratory water bath, and each sample was measured three times at each temperature.



**Figure 3.4:** Experimental setup in water bath for varying the temperature.

The cell constant of the Pyrex cell used in further calculations was determined from the impedance measurements of aqueous solutions with varying concentration and mixing ratios. A mean cell constant was calculated from the measured resistances and tabular conductivities as shown in Appendix A.

---

### 3.3 Molten salt

#### 3.3.1 Quartz cell design

For the high temperature measurements, a new test cell as shown in Figure 3.5 was designed in quartz to withstand the testing conditions. Quartz was chosen as the cell material because of its low thermal coefficient of expansion (CTE), with a CTE of approximately  $5.0 \times 10^{-7} \text{ }^\circ\text{C}^{-1}$  [58].

The cell design in quartz was modified from the Pyrex cell to fit the specifications of the crucible in the furnace. Still, the cell was designed with a U-shape to make the resistance in the tube dominant compared to the resistance in the reservoir.

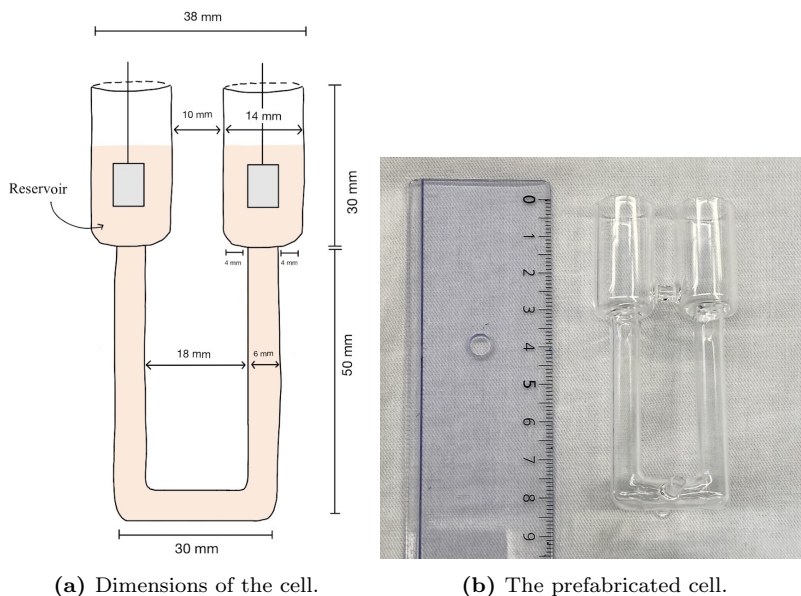


**Figure 3.5:** Dimensions and final product.

In order to ensure accurate measurements in the high temperature furnace, the cell constant of the quartz cell was determined at room temperature using the same method employed for aqueous solutions. After the experiments at high temperatures, the cell constant was measured again to confirm the consistency of the cell's performance during the high temperature measurements.

The cell constant of the quartz cell used in high temperature measurements was found by measuring the resistance of aqueous solutions. NaCl (1 M, 2 M) and KCl (1 M, 2 M) were measured at 25 °C, and a mean cell constant was calculated from

---

the measured resistances and tabular conductivities as shown in Appendix B.

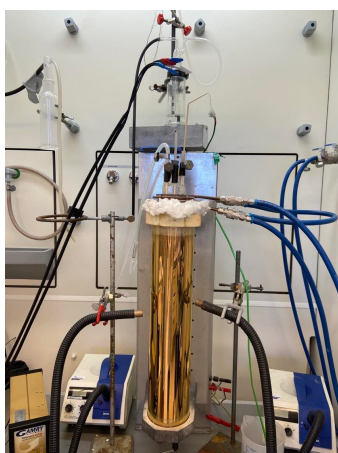
### 3.3.2 Impedance measurements with molten NaCl and KCl

The impedance of binary mixtures with various compositions of NaCl and KCl was measured at several temperatures above the melting point. The compositions studied were 50 mol% NaCl - 50 mol% KCl and 80 mol% NaCl - 20 mol% KCl. To ensure a similar liquid level throughout the different experiments, the density of the molten salt mixtures was used to determine the necessary mass of each salt. In every experiment, the total volume of the molten salt mixture was approximately 7 millilitres. A calculation example is shown in Appendix C.

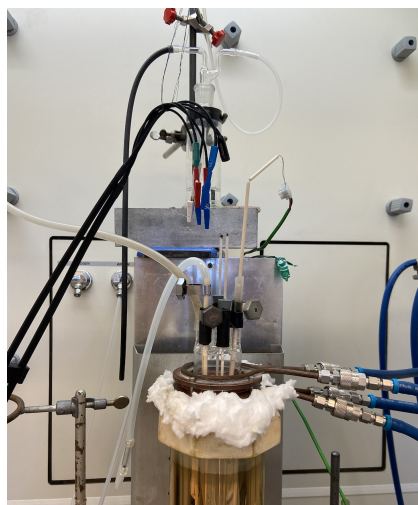
A gold-plated furnace was used to melt the salt mixtures to the desired temperature range. The advantages of choosing a gold-plated furnace are its transparency and thermal insulation properties. The customised cell containing the salt mixtures was placed in a bigger quartz crucible as shown in Figure 3.6 to ensure stability and prevent spills in the furnace. For improved temperature regulations within the furnace, a Type S Thermocouple was placed as close to the quartz cell as possible. Before melting, the salts were dried at 200 °C for 30 minutes. The temperature was then raised above the melting point of the mixtures, before the impedance of the melts was measured at increasing temperatures. Throughout the experiment, argon gas was circulating through the oven. A continuous flow of cooling water was streaming through the cooling loop interlinking the quartz crucible and its lid. The furnace setup is shown in Figure 3.7.



**Figure 3.6:** The setup of the customised cell inside the quartz crucible. The electrodes are covered in salt.



(a) The image displays the complete setup of the gold furnace, including water cooling, lighting, and electrodes.



(b) Close up of the setup, including the lid of the crucible.

**Figure 3.7:** The figures provide a total overview of the experimental setup for the gold furnace.

The same potentiostat used for impedance measurements of aqueous salt solutions, Gamry Reference 620 Potentiostat, was used for high temperature measurement at a frequency range between 1 MHz to 1 Hz. At each temperature, the impedance of the melt was measured three times. To better accommodate the quartz cell, the platinum electrodes previously used were replaced by a pair of electrodes with reduced surface area.

### 3.3.3 Impedance measurements of melts with hygroscopic compounds

The experimental arrangement used for the measurements of NaCl-KCl was also implemented for hygroscopic salts. To prevent the hygroscopic salts from reacting with moisture, the salts were weighed inside a glove box before being transferred to the gold furnace. In order to prevent any potential reaction between the salts and moisture present on the equipment, all items were placed in a drying cabinet the day prior to the experiments.

In the first experiment with  $\text{AlCl}_3$ , the salt was added first to the quartz cell, while the remaining salts were added on top. The initial idea was that placing  $\text{AlCl}_3$  at the bottom would prevent sublimation, and the salts would eventually mix together. However, when the temperature was increased, the  $\text{AlCl}_3$  turned dark, and the cell cracked. Because of this, a new approach had to be taken.

---

$\text{AlCl}_3$  is a highly hygroscopic salt that sublimates at approximately  $180\text{ }^\circ\text{C}$  [59]. To avoid this, first,  $\text{AlCl}_3$  and  $\text{NaCl}$  were melted at the eutectic composition at  $157^\circ\text{C}$ , composing  $\text{NaAlCl}_4$ . The homogeneous mixture was then cooled, crushed, and added in the correct composition with the other salts. The entire mixture was then added to the quartz cell inside a glove box to ensure that  $\text{AlCl}_3$  would not react with the moisture in the air. This approach was successful, resulting in a homogeneous mixture of melted salts. Figure 3.8 shows the mixed salts with added  $\text{AlCl}_3$ .



**Figure 3.8:** Crushed  $\text{NaAlCl}_4$  blended with  $\text{NaCl}$  and  $\text{KCl}$  in the quartz cell.

In the first experiment, the salt mixture consisted of a eutectic composition of  $\text{NaCl}$  and  $\text{KCl}$  with an addition of 8 mol%  $\text{AlCl}_3$ . Due to cell breakage during the execution, the composition was adjusted to contain 3 mol%  $\text{AlCl}_3$ . To achieve this, 0.865 g of the mixture containing crushed  $\text{NaAlCl}_4$ , equivalent to 3 mol% of  $\text{AlCl}_3$  in the total melt, was weighed out. The remaining 4.263 g  $\text{NaCl}$  and 5.439 g  $\text{KCl}$  were then added to obtain the desired composition, resulting in a total mass of 10.346 g in the quartz cell.

In the second experiment with  $\text{AlCl}_3$ ,  $\text{LiCl}$  was also added. For easier comparison between the two salt melts containing  $\text{AlCl}_3$ , the same mass as in the first experiment was weighed out, but with an additional 1 g of  $\text{LiCl}$ . This amount of  $\text{LiCl}$  corresponds to a molar fraction of 15.683 mol% in the total melt. Further details of the calculations can be found in Appendix D.

# 4 Results and Discussion

## 4.1 Aqueous solutions

### 4.1.1 Cell design

The U-shaped Pyrex cell had a narrow tube diameter, making the tube resistance dominant. Resistance in the reservoirs could therefore be considered negligible, thus minimising the impact of electrode positioning and liquid level variations in the reservoirs on the experimental outcomes. The measurements obtained with the cell demonstrated low deviations between each measurement of an aqueous solution, even when experiments were conducted on different days. Achieving low deviations is indicative of successful measurements as it shows precision of the method. In addition, the average standard deviation for the mean cell constant was calculated to  $(\pm) 0.147 \text{ cm}^{-1}$  as shown in Appendix A, increasing the reliability of the calculated cell constant. A similar cell design was therefore also used for the high temperature measurements.

### 4.1.2 Measurements at room temperature

The impedance measurements of aqueous electrolytes are presented in Nyquist plots. An example plot for KCl is shown in Figure 4.1 while additional plots can be found in Appendix E.

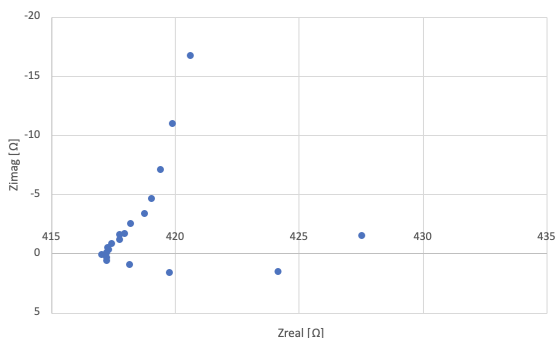


**Figure 4.1:** Nyquist plot of KCl (1 M) at 25 °C.

In order to determine  $R_s$ , the x-coordinate with the corresponding y-value closest to zero was chosen as the measured resistance. Further details are provided in Appendix E.

---

The average resistances and the associated conductivity for NaCl and KCl with various concentrations at 25 °C are presented in Table 4.1 and 4.2. All the measurements used to calculate the average resistances and the cell constant are listed in Appendix A along with an example of conductivity calculation. The calculation of the given standard deviations and percentage deviations can be found in Appendix F.

**Table 4.1:** Resistance measurements for salt solutions of NaCl and KCl with varying concentrations.

Electrolyte	Average measured resistance [ $\Omega$ ]	Standard deviation resistance [ $\Omega$ ]	Percentage deviation [%]
1 M NaCl	542.094	( $\pm$ ) 2.199	( $\pm$ ) 0.406
2 M NaCl	311.934	( $\pm$ ) 0.337	( $\pm$ ) 0.108
Saturated NaCl	185.239	( $\pm$ ) 0.258	( $\pm$ ) 0.447
1 M KCl	416.943	( $\pm$ ) 0.064	( $\pm$ ) 0.015
2 M KCl	226.880	( $\pm$ ) 0.614	( $\pm$ ) 0.271

**Table 4.2:** Resistance measurements and tabular conductivity for salt solutions of NaCl and KCl with varying concentrations.

Electrolyte	Calculated conductivity [S/cm]	Tabular conductivity values [S/cm], [60]
1 M NaCl	0.084 ( $\pm$ 0.405 %)	0.084
2 M NaCl	0.145 ( $\pm$ 0.108 %)	0.145
Saturated NaCl	0.245 ( $\pm$ 0.139 %)	-
1 M KCl	0.109 ( $\pm$ 0.015 %)	0.109
2 M KCl	0.200 ( $\pm$ 0.271 %)	0.199

From Table 4.1, it is recognised from the resistance deviation that the measured resistances within a sample exhibit a degree of variation. However, the results presented in Table 4.2 reveal a notable similarity between the experimentally determined conductivity values and their corresponding tabulated values. This finding serves as an indication of the effectiveness and precision of the methodology



---

in measuring conductivity. The variation of measured resistance may be due to slight temperature differences in the laboratory, disturbances on the electrodes such as air bubbles or differences in the experimental setup. The percentage deviations in measured resistances are under 1 % for all samples, but the slight uncertainty in the measurements still affects the calculated cell constant used in further measurements. A greater number of well-studied aqueous electrolytes used in calculation of the cell constant would have reduced the error further.

As seen in Table 4.2, KCl solutions exhibit a higher conductivity compared to NaCl despite  $K^+$ -ions having a greater ionic radius than  $Na^+$ -ions. This indicates that there are factors other than the original ionic radius influencing the ion's mobility and consequently the solution's conductivity. When dissolved in water, the cations become hydrated and less mobile. The KCl solutions having elevated conductivity illustrates that  $Na^+$  achieves a more stable hydration shell, resulting in a larger total ionic radius in comparison to  $K^+$ . This explains the disparity in conductivity between the two salt solutions [18].

The conductivities of NaCl solutions presented in Table 4.2 are plotted as a function of concentration in Figure 4.2. Saturated NaCl (approximately 6 M) is included in the figure.

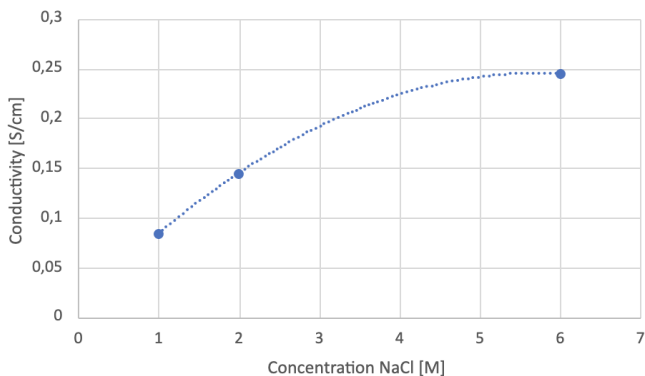


**Figure 4.2:** Conductivity of various NaCl concentrations at 25 °C.

As seen in Figure 4.2, the conductivity demonstrates a positive correlation with the concentration of NaCl. Once the concentration reaches higher levels, the conductivity displays a reduced rate of increase. This phenomena can be related to the decrease in ionic mobility caused by enhanced electrostatic interaction in the solution [21]. As the concentration increases, the lessened distance between the ions will contribute to more present Coulomb interactions between ions, limited mobility

---

and possibly formation of non-conductive ion pairs, explaining the reduced rate of conductivity increase [13], [24].

NaCl (1 M) and KCl (1 M) were mixed together in several ratios to investigate the effect on conductivity. In addition to calculating conductivity based on measured resistance, conductivity values were calculated on basis of the obtained conductivity values of single salt solutions and their mixing ratio. The calculations are presented in Appendix A, while the results are presented in Table 4.3. This was done to investigate if there are other factors than the salt concentrations contributing to the conductivity in mixed salt electrolytes.

**Table 4.3:** Comparison of tabular and calculated conductivity, in addition to conductivity calculated from various mixing ratios.

Electrolyte [mol%]	Tabular conductivity values [S/cm], [25]	Calculated conductivity [S/cm]	Conductivity calculated from mixing ratios [S/cm]
50-50 KCl-NaCl	-	0.097	0.096
20-80 KCl-NaCl	0.089	0.089	0.089
80-20 KCl-NaCl	0.104	0.105	0.104
40-60 KCl-NaCl	0.094	0.095	0.094
60-40 KCl-NaCl	0.099	0.098	0.099

The conductivity of the solution was clearly dependent on the mixing ratio of NaCl and KCl. KCl (1 M) has a higher conductivity than NaCl (1 M), and addition of NaCl (1 M) therefore decreases the conductivity. Because of the consistent decline in conductivity when adding more NaCl (1 M), the shift in conductivity might be due to the decreasing concentration of KCl alone. A concentration of 1 M in the solutions may not be sufficient to consider other factors such ionic interactions and their influence that could arise from the different cations present in the solutions. As for the conductivities calculated from the mixing ratios, Table 4.3 shows that these values are in complete agreement with the tabulated conductivities. The calculations are therefore a valuable method to estimate the conductivity of a mixed aqueous solution at lower concentrations.

---

### 4.1.3 Measurements at varying temperature

The graph in Figure 4.3 shows the correlation between the conductivity of NaCl (1 M) and KCl (1 M) and temperature between 25 °C and 50 °C. The results indicate a positive correlation between temperature and conductivity, with an increase in temperature leading to a corresponding increase in conductivity. The resistance measurements used to calculate the conductivities in the plot are given in Appendix G.

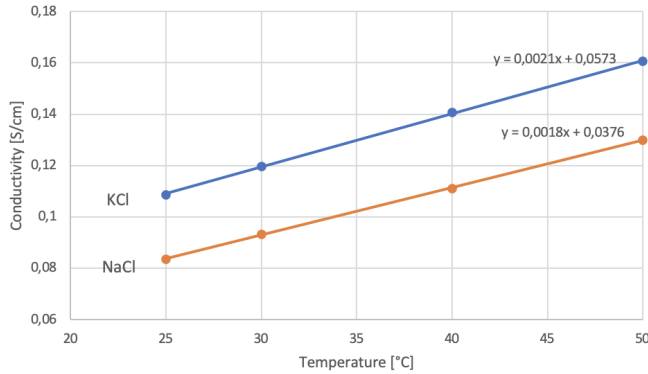


**Figure 4.3:** Conductivity [ $\frac{S}{cm}$ ] for NaCl (1 M) and KCl (1 M) plotted against temperature [°C].

The plot illustrates a linear relationship between temperature and the calculated conductivity, where an increase in temperature is associated with an increase in conductivity. The observed increase in conductivity may be caused by the reduction in intermolecular forces, which will enhance the ion migration. Higher temperatures will also decrease the viscosity of the water, further enhancing the ion mobility [13].

By plotting the natural logarithm of calculated conductivity as a function of the inverse temperature, the Arrhenius plot is obtained. From the Arrhenius plot, the activation energy  $E_a$  can be determined from the slope of the graph as shown in Equation 2.7.

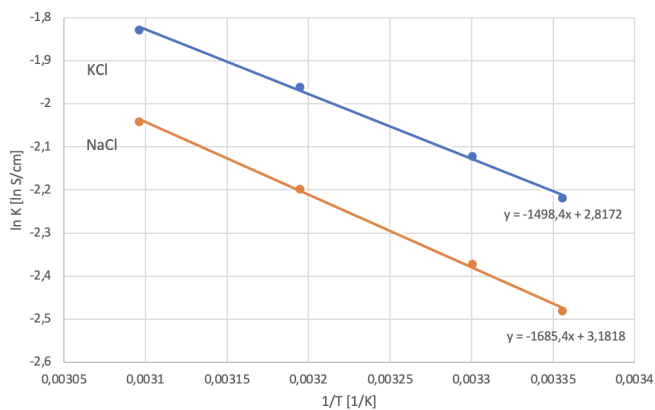


**Figure 4.4:** Arrhenius plot for NaCl (1 M) and KCl (1 M) in aqueous solutions.

In Figure 4.4, the y-axis represents the natural logarithm of the calculated conductivity, and the x-axis represents the reciprocal to the temperature in Kelvin. The activation energies  $E_a$  for KCl (1 M) and NaCl (1 M) were determined to be  $12.457 \frac{\text{kJ}}{\text{mol}}$  and  $14.012 \frac{\text{kJ}}{\text{mol}}$  respectively. The observed increase in  $E_a$  from KCl to NaCl agrees with the lower conductivity for NaCl.

---

## 4.2 Molten salts

The following results present the measured resistances and calculated conductivities of melts with varying composition of NaCl, KCl, LiCl and AlCl<sub>3</sub>. Each salt melt was analysed within the 700-800°C temperature range, and the conductivity was plotted as a function of temperature.

The main focus during the experimental investigations was centred on evaluating the impact of varying AlCl<sub>3</sub> and LiCl compositions, and how these affect the conductivity of the electrolyte. KCl was selected as an additive because of its ability to lower the melting point of a NaCl melt when mixed in eutectic composition. In addition, KCl is easy to work with, has much available literature data and is inexpensive. However, it should be noted that KCl is not a likely option for industrial processes as it may shorten the service life of the graphite cathode, possibly due to intercalation of potassium expanding the graphite crystal lattice [61].

### 4.2.1 Cell design

The experimental setup was not specifically optimised for the gold furnace, and some challenges were encountered during the experiments. For instance, it was difficult to prevent the quartz cell from sliding within the quartz crucible, which at times made it challenging to ensure a consistent electrode placement in each experiment. Despite these challenges, the experimental setup was still able to yield valuable results.

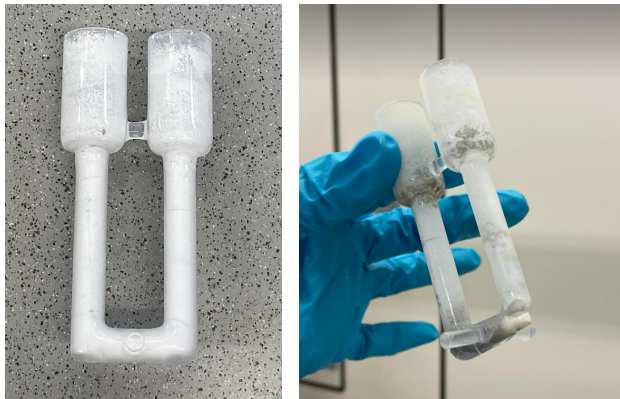


**Figure 4.5:** The quartz cell containing molten NaCl-KCl with eutectic composition inside the furnace.

---

Figure 4.5 shows how the quartz cell containing molten salt placed in the furnace. It is noticeable that during the lowering of the electrodes into the salt, one of them became dislocated from its intended position. However, this should not affect the results significantly due to the cell's U-shape.

During the course of experiments, issues with the quartz cell appeared after the third experiment. The glass turned opaque and developed a white layer that was impossible to remove, covering the interior of the cell. This posed a challenge during the experimental setup, as the opaque cell made it impossible to see the electrode position. Throughout the course of the fourth experiment, the quartz cell fractured when the salt mixture was molten, causing the molten salt mixture to leak into the surrounding quartz crucible. The fracture of the cell may have been a result of repetitive damaging interactions with the molten salts. Figure 4.6a and 4.6b shows the damages after use. When quartz glass is used in a molten salt environment the ions in the melt will diffuse into the glass, causing devitrification. The ion diffusion will cause changes in the glass composition, ultimately resulting in the glass becoming opaque or even shattered [62].



(a) The opaque quartz cell after the third experiment. (b) The fractured cell after the fourth experiment.

**Figure 4.6:** Cell damages.

Considering that the quartz cell fractured during the fourth experiment, the experimental procedure may not be sustainable for multiple experiments due to the observed effects of molten chloride salts on quartz glass. Consideration should be given to the use of more corrosive resistant construction materials if repeated use of the U-shaped cell is required. This material does not necessarily have to be transparent.

---

Because the first quartz cell fractured, a new cell was utilised for the remaining experiments. As the quartz cells' dimensions differed slightly, two separate cell constants were determined. The value of the cell constant found for the first quartz cell was determined to be  $42.258 \text{ cm}^{-1}$ , and this cell was used in the measurements of eutectic composition of NaCl-KCl, 80-20 mol% NaCl-KCl and eutectic composition NaCl-KCl added 20 mol% LiCl. The cell constant for the second quartz cell used for measurements of molten salts mixtures containing  $\text{AlCl}_3$  was determined to be  $39.671 \text{ cm}^{-1}$ . The calculation of both cell constants are shown in Appendix B. The cell constants were determined from measurements of four individual aqueous solutions, but to strengthen the accuracy of the cell constants, it is recommended to complete further measurements on additional solutions. Other factors that may influence the cell constants are the presence of resistance in the cord, which can lead to higher resistance measurements. The sum of the resistance of the two platinum cords was measured at room temperature and considered to be negligible to the total resistance in measurements of aqueous solutions. However, the increase of temperature in molten salt measurements may increase the cord resistance, resulting in a higher impact on the calculated conductivities of molten salt mixtures [63]. This might cause greater errors related to cord resistance in the high temperature measurements.

Following the fracture of the first quartz cell, it was desirable to investigate whether the geometry of the second cell was affected by the chloride salts during the experiments, potentially altering the cell constant. After the last high temperature experiment, the cell constant was determined again from measurements of the same aqueous solutions previously used. There were insignificant changes in the cell constant, increasing the reliability of the high temperature measurements.

#### **4.2.2 Eutectic composition of NaCl-KCl**

50-50 mol% NaCl-KCl was chosen as a molten salt composition because it is equivalent to the eutectic composition of NaCl and KCl. Here, the melting point is only  $657 \text{ }^\circ\text{C}$ , which is favourable for the experimental work and temperature range studied [64]. The resistance of 50-50 mol% NaCl-KCl was measured at  $700 \text{ }^\circ\text{C}$ ,  $750 \text{ }^\circ\text{C}$  and  $800 \text{ }^\circ\text{C}$ , and is presented in Table 4.4 along with the calculated conductivities. The standard and percentage deviations were calculated as shown in Appendix F, and the measurements used to obtain the mean resistances are presented in Appendix H.

**Table 4.4:** Resistance measurements and associated conductivity for eutectic NaCl-KCl composition at varying temperatures.

Temperature [°C]	Average measured resistance [ $\Omega$ ]	Calculated conductivity [ $\frac{S}{cm}$ ]	Tabular conductivity [S/cm], [65]
700	18.750 ( $\pm$ 0.005 $\Omega$ )	2.254 ( $\pm$ 0.026 %)	2.331
750	17.718 ( $\pm$ 0.010 $\Omega$ )	2.387 ( $\pm$ 0.059 %)	2.487
800	16.909 ( $\pm$ 0.006 $\Omega$ )	2.500 ( $\pm$ 0.038 %)	2.630

The results presented in Table 4.4 show an evident similarity between the measured and tabulated conductivity, indicating a successful performance of the developed method and the functionality of the designed cell. Still, a minor discrepancy was observed between calculated conductivity and the tabulated values, as the calculated conductivities were lower. The discrepancy may be caused by several factors. Firstly, it should be noted that the tabulated values used for comparison are given for a composition of 51.23 mol% NaCl. Secondly, the electrode cord resistance might negatively influence the calculated conductivities in the experiments with molten salts. Despite the minor deviations, the experimental results are still considered adequate, and further calculated conductivities of the remaining molten salt compositions will not be compared to tabular values due to limited availability.

The conductivities presented in Table 4.4 are plotted as a function of temperature in Figure 4.7. In the temperature range 700-800 °C, the conductivity of 50-50 mol% NaCl-KCl increases almost linearly, as seen in Figure 4.5.

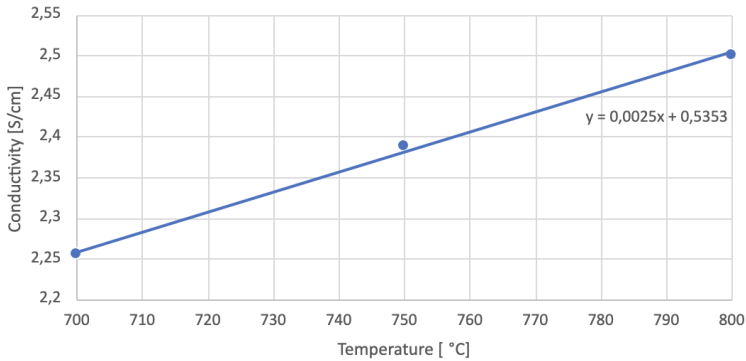


**Figure 4.7:** The conductivity of molten NaCl-KCl with eutectic composition plotted as a function of temperature.



---

The increase in conductivity is caused by an increased ion mobility at higher temperatures. An increased temperature causes the ions to move at greater velocities, resulting in a higher conductivity [31].

#### 4.2.3 80-20 mol% NaCl-KCl

To investigate the impact of the individual salts on the conductivity of the salt melt, the resistance of molten NaCl and KCl with a composition of 80-20 mol% was analysed. This composition has a higher melting point than the eutectic mixture, and the molten mixture was therefore analysed in the temperature range 730-800 °C. The measured resistances and calculated conductivities are presented in Table 4.5, and the measurements used to obtain the mean resistances are presented in Appendix H.

**Table 4.5:** Average measured resistance and associated conductivity values for a solution containing 80 mol% NaCl and 20 mol% KCl at varying temperatures.

Temperature [°C]	Average measured resistance [ $\Omega$ ]	Calculated conductivity [S/cm]
<b>730</b>	15.309 ( $\pm$ 0.002 $\Omega$ )	2.760 ( $\pm$ 0.011 %)
<b>750</b>	15.021 ( $\pm$ 0.003 $\Omega$ )	2.813 ( $\pm$ 0.020 %)
<b>770</b>	14.774 ( $\pm$ 0.002 $\Omega$ )	2.860 ( $\pm$ 0.015 %)
<b>800</b>	14.440 ( $\pm$ 0.002 $\Omega$ )	2.927 ( $\pm$ 0.015 %)

When comparing Table 4.4 and 4.5, it is evident that a lower mol% KCl gives a better conductivity than 80-20 mol% NaCl-KCl. In contrast to aqueous solutions, where KCl displayed better conductivity, NaCl has a better conductivity in molten salts. This is attributed to the absence of water, which prevents the formation of hydration shells. In salt melts, the size of the ion is the decisive factor [33]. Na<sup>+</sup>-ions holds a smaller ionic radius than K<sup>+</sup>-ions, which results in a superior electrical conductivity.

The conductivities presented in Table 4.5 is plotted as a function of temperature in Figure 4.8. In the given temperature range, there is a nearly linear increase in conductivity as observed in the 50-50 mol% NaCl-KCl melt, which again can be linked to increased ion mobility [31].

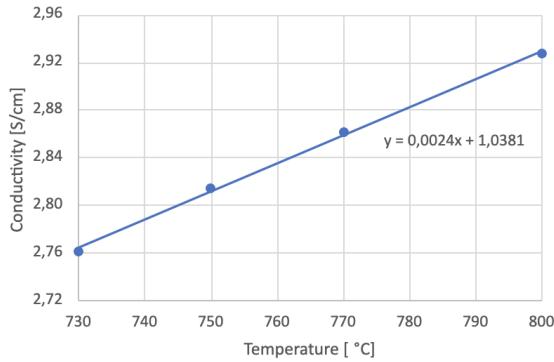


**Figure 4.8:** The conductivity of 80-20 mol% NaCl-KCl plotted as a function of temperature.

#### 4.2.4 Eutectic composition of NaCl-KCl + 20 mol% LiCl

It was desirable to investigate the impact of addition of LiCl to a NaCl-KCl melt, as  $\text{Li}^+$ -ions have a small ionic radius and should therefore be more mobile than both  $\text{Na}^+$  and  $\text{K}^+$  [33]. An equimolar composition of NaCl and KCl was selected as the base composition due to the presence of its eutectic point lowering the melting point, hence simplifying the experimental work. The total molten mixture consisted of 20 mol% LiCl, and the measured resistances and calculated conductivities are shown in Table 4.6. The measurements used to obtain the mean resistances are presented in Appendix H.

**Table 4.6:** Average measured resistance and associated conductivity values for a solution containing eutectic composition of NaCl-KCl added 20 mol% LiCl at varying temperatures.

Temperature [°C]	Average measured resistance [ $\Omega$ ]	Calculated conductivity [S/cm]
700	17.301 ( $\pm 0.011 \Omega$ )	2.443 ( $\pm 0.063 \%$ )
730	16.747 ( $\pm 0.005 \Omega$ )	2.523 ( $\pm 0.029 \%$ )
750	16.391 ( $\pm 0.004 \Omega$ )	2.578 ( $\pm 0.025 \%$ )
770	16.091 ( $\pm 0.003 \Omega$ )	2.626 ( $\pm 0.018 \%$ )
800	15.659 ( $\pm 0.014 \Omega$ )	2.699 ( $\pm 0.092 \%$ )

In comparison to the eutectic composition of NaCl-KCl, the addition of LiCl attributes positively to the conductivity of the melt. As  $\text{Li}^+$ -ions have smaller

---

atomic radii than  $\text{Na}^+$  and  $\text{K}^+$ ,  $\text{Li}^+$ -ions are more mobile, positively affecting the conductivity [31]. The conductivities presented in Table 4.6 is plotted as a function of temperature in Figure 4.9. Again, the conductivity increases linearly with an increasing temperature.

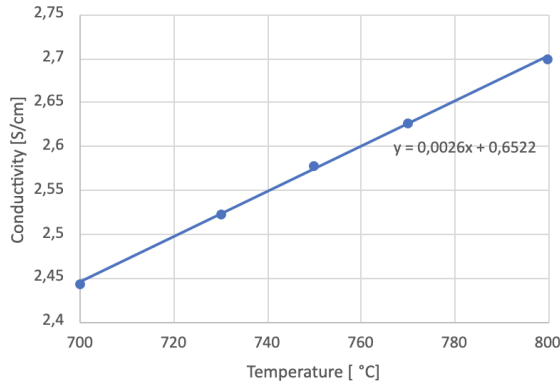


**Figure 4.9:** The conductivity of the eutectic composition of NaCl-KCl added 20 mol% NaCl-KCl-LiCl plotted as a function of temperature.

#### 4.2.5 Eutectic composition of NaCl-KCl + 3 mol% $\text{AlCl}_3$

The inclusion of  $\text{AlCl}_3$  to the eutectic composition of NaCl and KCl caused additional experimental challenges. Even though  $\text{AlCl}_3$  was handled attentively in the glove box before melting, there were indications of contamination of the salt. In the initial attempt of melting NaCl, KCl and  $\text{AlCl}_3$ ,  $\text{AlCl}_3$  of 98 % purity was placed in the tube of the quartz cell and covered with a eutectic composition of NaCl and KCl. Upon heating, the formation of black particles was observed in the tube, clearly emerging from  $\text{AlCl}_3$ . This indicates that the salt used was impure, and in further experiments a new batch of  $\text{AlCl}_3$  was used. Figure 4.10 illustrates the presence of impurities present after the experiment, which is revealed as dark particles observed on the inner surface of the cell.

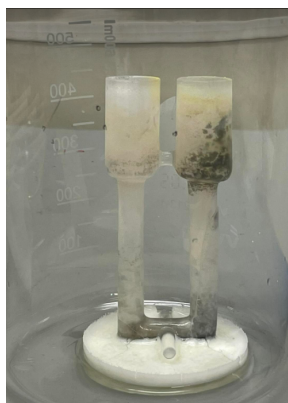


**Figure 4.10:** Evidence of contamination seen in the quartz cell after the first experiment with  $\text{AlCl}_3$ .

From Figure 4.10, the specific source of contamination resulting in formation of the dark particles remains unclear. However, the dark colour might indicate traces of moisture.  $\text{AlCl}_3$  is usually a colourless-to-white powder that becomes grey-to-yellow when exposed to moisture [66]. The salt may have been exposed to moisture on multiple occasions, despite efforts made to prevent it.  $\text{AlCl}_3$  could have absorbed moisture from the surrounding environment. Most of the procedure was carried out within a glove box, but the assembly itself had to be performed outside of it.

In addition to contamination, achieving a homogeneous melt of the three salts posed a challenge. It was unclear whether  $\text{AlCl}_3$  melted together with  $\text{NaCl}$  or sublimated as the sublimation temperature of  $\text{AlCl}_3$  is about  $180\text{ }^\circ\text{C}$ , and there was no sign of the salt mixture melting before approximately  $700\text{ }^\circ\text{C}$ . Instead, the lid of the quartz crucible rapidly filled with white vapour as shown in Figure 4.11, which led to the suspicion that  $\text{AlCl}_3$  had sublimated. This could also be evaporation of the other salts.



**Figure 4.11:** White coating seen inside the top of the crucible after the experiment.

To ensure the melting of  $\text{AlCl}_3$  in the following experiments,  $\text{AlCl}_3$  was mixed together with  $\text{NaCl}$  in a 50-50 mol% composition and melted before dried and crushed into a homogeneous salt mixture. Since the melting point of the composition of  $\text{AlCl}_3$  and  $\text{NaCl}$  is below the sublimation temperature of  $\text{AlCl}_3$ , the salt will fuse without loss of  $\text{AlCl}_3$  [35]. The formed homogeneous salt mixture was then easier to use in further experiments.



**Figure 4.12:** The product obtained after melting 50-50 mol%  $\text{NaCl-AlCl}_3$  to a homogeneous mixture at 170 °C.

Figure 4.12 shows that the melted salt became dark grey-yellow when melted at 170 °C, and had a crystalline structure.  $\text{NaAlCl}_4$  was crushed into fine particles inside a glove box to prevent the salt from absorbing moisture from the environment. It was then added to the eutectic mixture of  $\text{NaCl}$  and  $\text{KCl}$ . The ternary mixture was then transferred into the quartz cell, and the melting and conductivity measures were carried out without further complications. The measured resistances and conductivities of the molten salts are presented in Table 4.7, and the measurements used to obtain the mean resistances are presented in Appendix H.

**Table 4.7:** Average measured resistance and associated conductivity values for eutectic NaCl-KCl added 3 mol% AlCl<sub>3</sub>.

Temperature [°C]	Average measured resistance [ $\Omega$ ]	Calculated conductivity [S/cm]
700	19.975 ( $\pm$ 0.034 $\Omega$ )	1.986 ( $\pm$ 0.170 %)
730	19.291 ( $\pm$ 0.027 $\Omega$ )	2.066 ( $\pm$ 0.139 %)
750	18.732 ( $\pm$ 0.017 $\Omega$ )	2.118 ( $\pm$ 0.089 %)
770	18.316 ( $\pm$ 0.014 $\Omega$ )	2.166 ( $\pm$ 0.074 %)
800	17.742 ( $\pm$ 0.055 $\Omega$ )	2.236 ( $\pm$ 0.055 %)

In comparison to the eutectic composition of molten NaCl-KCl, the addition of AlCl<sub>3</sub> attributes negatively to the conductivity of the melt. This is due to the strong attractive force between Al<sup>3+</sup> and Cl<sup>-</sup> existing in a melt, forming complex groupings such as [AlCl<sub>4</sub><sup>-</sup>] and [Al<sub>2</sub>Cl<sub>7</sub><sup>-</sup>] [35]. These complexes are bigger and therefore less mobile, leading to a loss in conductivity.

As in previous experiments, the conductivity increases linearly with increasing temperature as shown in Figure 4.13.

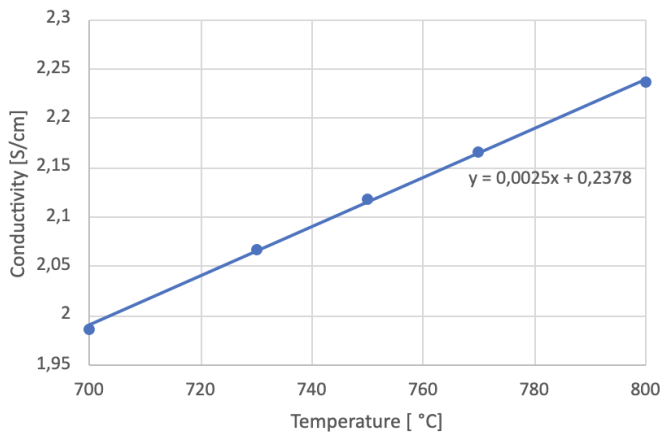


**Figure 4.13:** The conductivity of eutectic NaCl-KCl composition with 3 mol% AlCl<sub>3</sub> added plotted as a function of temperature.

---

#### 4.2.6 Eutectic composition of NaCl-KCl + 3 mol% AlCl<sub>3</sub> + 1 g LiCl

During the melting of the eutectic composition of NaCl-KCl added AlCl<sub>3</sub> and LiCl, it was observed that this composition had a lower melting point compared to the sample that did not contain LiCl. The mixture began to liquefy at 600 °C and was nearly entirely liquid by 650 °C. A lower melting point might be beneficial in various industrial applications as it requires less energy for melting. However, the high costs of LiCl it is necessary to find an optimal balance between the expenses of LiCl and energy usage. The measured resistances and associated conductivities of the melt are presented in Table 4.8, and the measurements used to obtain the mean resistances are presented in Appendix H.

**Table 4.8:** Average measured resistance and associated conductivity values for eutectic NaCl-KCl added 3 mol% AlCl<sub>3</sub> and 1 g LiCl.

Temperature [°C]	Average measured resistance [ $\Omega$ ]	Calculated conductivity [S/cm]
700	19.043 ( $\pm$ 0.0319 $\Omega$ )	2.083 ( $\pm$ 0.098 %)
730	18.349 ( $\pm$ 0.006 $\Omega$ )	2.162 ( $\pm$ 0.031 %)
750	17.942 ( $\pm$ 0.009 $\Omega$ )	2.211 ( $\pm$ 0.049 %)
770	17.545 ( $\pm$ 0.006 $\Omega$ )	2.261 ( $\pm$ 0.032 %)
800	17.059 ( $\pm$ 0.019 $\Omega$ )	2.326 ( $\pm$ 0.111 %)

The addition of LiCl to the NaCl-KCl-AlCl<sub>3</sub> melt enhanced the melt's conductivity as predicted. Li<sup>+</sup>-ions have a greater polarising strength than Na<sup>+</sup> and K<sup>+</sup>, thus weakening the bonds in the [AlCl<sub>4</sub><sup>-</sup>] and [Al<sub>2</sub>Cl<sub>7</sub><sup>-</sup>] complex grouping [38]. This will increase the activity of AlCl<sub>3</sub> in the melt and further enhance the melt's conductivity.

Similar to previous experiments, the conductivity displays a linear increase with a rise in temperature as seen in Figure 4.14.

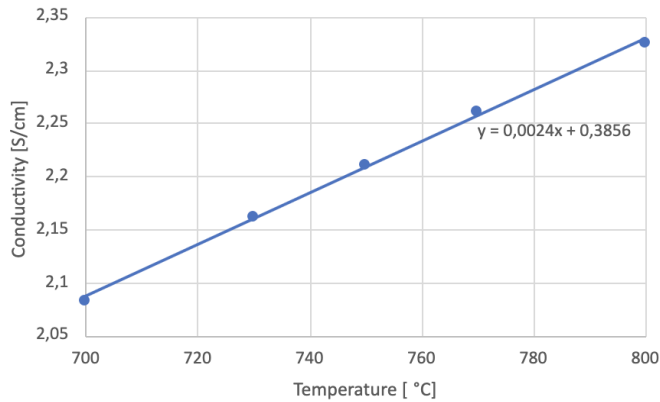


**Figure 4.14:** The conductivity of eutectic NaCl-KCl added 3 mol% AlCl<sub>3</sub> and 1 g of LiCl plotted as a function of temperature.

#### 4.2.7 Comparison of conductivity and activation energy for all molten salt compositions

The conductivity as a function of temperature for all molten salt compositions is presented together in Figure 4.15.

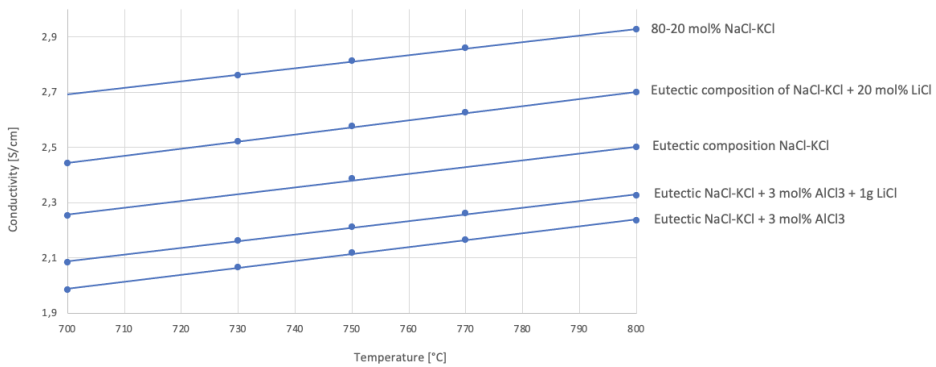


**Figure 4.15:** Comparison of all conductivity measurements of molten salt mixtures as a function of temperature.

As evidenced by the data presented in 4.15, the samples containing AlCl<sub>3</sub> exhibit the lowest conductivity levels, whereas the inclusion of LiCl results in increased conductivity values. Still, the composition 80-20 mol% NaCl-KCl clearly has the highest conductivity, indicating that the size of K<sup>+</sup> significantly affects the conductivity. The molten salt compositions with higher proportion of cations



having smaller atomic radii exhibit noticeably higher conductivity. The outcomes therefore align with the anticipated results.

The conductivity increases linearly with increasing temperature. This might not be the case for all temperature intervals, and it would therefore have been beneficial to study a larger range of temperature.

The activation energies of the various molten salt mixtures were obtained by plotting their respective Arrhenius plot. The plot is presented in Figure 4.16.

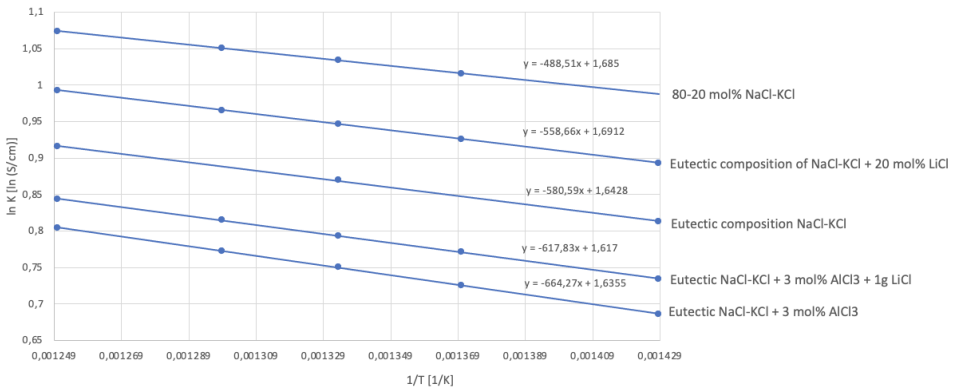


**Figure 4.16:** Arrhenius plot for all molten salt mixtures.

From Figure 4.16, it can be seen that the plotting of  $\ln(\kappa)$  versus  $\frac{1}{T}$  are essentially linear for the given temperature range. The corresponding activation energies calculated from Equation 2.7 are listed in Table 4.9.

**Table 4.9:** The activation energies for the various molten salt composition.

Melt composition	Activation energy [ $\frac{kJ}{mol}$ ]
80-20 mol% NaCl-KCl	4.061
Eutectic NaCl-KCl + 20 mol% LiCl	4.644
Eutectic NaCl-KCl	4.827
Eutectic NaCl-KCl + 3 mol% AlCl <sub>3</sub> + 1 g LiCl	5.136
Eutectic NaCl-KCl + 3 mol% AlCl <sub>3</sub>	5.523

As indicated in Table 4.9, the activation energies of the various melts exhibit clear

---

variations, with a difference of  $1.5 \frac{\text{kJ}}{\text{mol}}$  between the highest and lowest values. For alkali chloride salts, a decreasing ratio of anion to cation radius will increase the activation energy [39]. This can also be seen from the calculated activation energies in Table 4.9. Cations with smaller radii require less energy to migrate through the melt [39]. The molten salt mixture with the lowest activation energy, 80-20 mol% NaCl-KCl, has a high concentration of smaller cations. Additionally, molten salt mixtures containing LiCl, whose cation is small and mobile, also exhibit lower activation energies. Conversely, an increase in the concentration of  $\text{K}^+$  ions in the mixture hugely raises the activation energy, clearly demonstrating the impact of cation size. The molten salts containing  $\text{AlCl}_3$  also exhibit a distinct increase in activation energy, which could be attributed to the complex formation induced by  $\text{AlCl}_3$ . The bigger complexes are known to have lower mobility, which could explain this behaviour. The addition of LiCl to the  $\text{AlCl}_3$  composition decreases the activation energy, as the  $\text{Li}^+$ -ions weakens the bonds in the aluminium complexes [38].

Compared to the activation energies of KCl (1 M) and NaCl (1 M) presented in Table 4.4, the activation energies of the molten salts were significantly lower. This finding is consistent with the observed conductivities of the salt melts and aqueous solutions, as the molten salts exhibited 10-50 times higher conductivity values than the aqueous solutions [32].

### 4.3 Sources of Error

There are several sources of error that may occur when measuring conductivity in both aqueous solutions and molten salts.

#### 4.3.1 Uncertainties for the conductivity measurements in aqueous solutions

- Conductivity is a temperature-dependent property, and variations in temperature can affect the measurement accuracy. It is therefore necessary to measure the temperature to maintain a constant temperature throughout the experiment.
- Incorrect positioning of the electrodes in the solution and inconsistent amount of salt solution can lead to inaccurate measurements. It is crucial to ensure that the electrodes are fully immersed in the solution and spaced appropriately. To minimise the importance of electrode placement and level of salt solution, the cell was designed in a way that made the placement of electrodes less significant.

- 
- If there is a time delay between preparing the solution and taking the measurement, it can lead to changes in concentration and thereby conductivity due to evaporation of the solution.
  - Impurities on the electrode surface can affect the conductivity measurement. Therefore, it is essential to ensure that the electrodes are free from contamination before the measurement.
  - In order to increase the accuracy of determining the cell constant, a greater number of samples would be preferable to calculate the mean. This would provide a higher degree of certainty. To evaluate the accuracy of the cell constant, it may be beneficial to run tests on various solutions and compare the outcomes with tabular values.

#### 4.3.2 Uncertainties for the conductivity measurements in molten salts

- Hygroscopic salts are highly reactive and can easily react with atmospheric gases and moisture, leading to contamination affecting the conductivity measurements.
- Temperature gradients can develop within the molten salt or in the furnace, leading to variations in conductivity measurements. The temperature of the molten salt should therefore be maintained at a constant temperature throughout the measurement process.
- The electrodes long cord may introduce resistance that can impact the accuracy of the measurements. If the resistance of the electrodes is not taken into account during conductivity measurements, the measured resistance may be higher than the actual resistance of the electrolyte, leading to smaller values for the conductivity. In the presented values of measured resistance, the cord resistance is not taken into account because of uncertainties considering its magnitude.
- During the experiments with  $\text{AlCl}_3$ , a white coating was observed on the top of the crucible lid. The composition of this substance remains unknown, but it is possible that some of the  $\text{AlCl}_3$  may have evaporated and condensed on the lid. If this is the case, the conductivity of the solution would increase. However, it would be difficult to conclude with this hypothesis, as rising temperature is also a factor that contributes to increased conductivity.

## 5 Conclusion

Impedance measurements have been used to obtain the conductivity of aqueous solutions and salt melts of various salt compositions. Main conclusions that can be drawn from the experiments are summarised below.

- While KCl exhibits higher conductivity than NaCl in aqueous solutions, the opposite is observed in salt melts. The reason for this is the hydration shell  $\text{Na}^+$  forms in water.
- The experimental findings in salt melts indicate that  $\text{AlCl}_3$  and KCl contribute to a decrease in conductivity, while NaCl and LiCl result in an increase in conductivity.
- The U-shaped cell design provided high precision measurements. However, due to wear damage and the corrosive nature of chloride salts, quartz is not the optimal material for a cell repeatedly utilised at high temperatures.
- Performing experiments with  $\text{AlCl}_3$  in salt melts poses challenges due to its low sublimation temperature. The making of  $\text{NaAlCl}_4$  results in  $\text{AlCl}_3$  exhibiting lower hygroscopicity and reactivity towards moisture in the surroundings, rendering it more manageable in practical applications.
- The similarity in cell constant before and after the chloride salt experiments conducted in a high-temperature oven suggests that there was no alteration in the quartz cell's geometry during the experiments. This verifies the precision of the results.
- In industrial applications, a compromise between the salts that exhibit high and low conductivity is necessary, as  $\text{AlCl}_3$  is a crucial component in aluminium production and LiCl is a costly option. Melting points of the salt mixtures should also be considered.

---

---

## 6 Further Work

- If it is necessary to reuse the test cell multiple times, a material that can withstand corrosive alkali salts better than quartz should be considered.
- To avoid impurities in the salt melts, all handling of  $\text{AlCl}_3$  should be done inside a glove box to prevent  $\text{AlCl}_3$  from reacting with moisture in the surroundings. Ideally, this also includes the installation of the setup before transferring to the furnace.
- It is recommended to conduct experiments over a broader temperature range, allowing for a more comprehensive analysis of conductivity variations as a function of temperature.
- To determine the best cell constant possible, there should be implemented more individual experiments with a wider range of well-studied salt concentrations into the calculations.
- The composition of the salt should be checked after the experiments to determine if any sublimation of  $\text{AlCl}_3$  has occurred. Due to time limitations, this could not be prioritised.
- Considering that the main focus of this task was to study trends in conductivity for different compositions of alkali salts, the influence of cord resistance on the results is insignificant. However, if obtaining accurate conductivity values is crucial, it is important to acknowledge the impact of cord resistance. Specifically, the fact that resistance in the cord increases with increasing temperature should be taken into account.

---

## References

- [1] M. Reverdy and V. Potocnik, “History of Inventions and Innovations for Aluminium Production,” *TMS 2020 149th Annual meeting and Exhibition Supplemental Proceedings*, pp. 1895–1910, 2020.
- [2] Wayne H. Cotten, *The Alcoa Smelting Process at Anderson County Texas*, 2018.
- [3] J. Haraldsson and M. T. Johansson, “Review of measures for improved energy efficiency in production-related processes in the aluminium industry – From electrolysis to recycling,” *Renewable and Sustainable Energy Reviews*, vol. 93, pp. 525–548, 2018.
- [4] K. Grjothei, C. Krohn, and H. Øye, “Improvements to the Hall-Héroult Process for Aluminium Electrowinning,” *Trends in Electrochemistry*, pp. 373–374, 1977.
- [5] D. Hodgson and T. Vass, “Aluminium – Analysis - IEA,” 9 2022. [Online]. Available: <https://www.iea.org/reports/aluminium#>
- [6] E. Bjørlo, “Electrochemical Study of Aluminum Chloride in Basic Chloride Melts with Oxide Additions,” NTNU, Trondheim, Tech. Rep., 2020.
- [7] Y. Borisoglebskii, M. Vetyukov, and Z. Shatova, “Thermodynamic Activity of Aluminium Chloride in the Melts of Chlorides of Alkali and Alkali-Earth Metals,” *ResearchGate*, 1 1991. [Online]. Available: [https://www.researchgate.net/publication/236179087\\_Thermodynamic\\_Activity\\_of\\_Aluminium\\_Chloride\\_in\\_the\\_Melts\\_of\\_Chlorides\\_of\\_Alkali\\_and\\_Alkali-Earth\\_Metals](https://www.researchgate.net/publication/236179087_Thermodynamic_Activity_of_Aluminium_Chloride_in_the_Melts_of_Chlorides_of_Alkali_and_Alkali-Earth_Metals)
- [8] K. Hofstad, “Konduktans – Store norske leksikon,” 2023. [Online]. Available: <https://snl.no/konduktans>
- [9] —, “Konduktivitet– Store norske leksikon,” 2022. [Online]. Available: <https://snl.no/konduktivitet>
- [10] Gamry Instruments, “Basics of Electrochemical Impedance Spectroscopy.”
- [11] B. Pedersen, “Elektrolytisk dissosiasjon ,” 2020. [Online]. Available: [https://snl.no/elektrolytisk\\_dissosiasjon](https://snl.no/elektrolytisk_dissosiasjon)



- 
- [12] M. Silberberg, *Principles of General Chemistry*. McGraw-Hill Companies, 2007.
- [13] W. Zhang, X. Chen, Y. Wang, L. Wu, and Y. Hu, “Experimental and Modeling of Conductivity for Electrolyte Solution Systems,” *ACS Omega*, vol. 5, no. 35, p. 22465, 9 2020. [Online]. Available: [/pmc/articles/PMC7482292//pmc/articles/PMC7482292/?report=abstracthttps://www.ncbi.nlm.nih.gov/pmc/articles/PMC7482292/](https://pubs.acs.org/doi/10.1021/acso.3c01111)
- [14] P. Andersen and H. Fjellvåg, “Elektrolytter,” 2020. [Online]. Available: [https://snl.no/elektrolytter-\\_elektrokjemi](https://snl.no/elektrolytter-_elektrokjemi)
- [15] Mr. Jnanendra Chandra Ghosh, “The abnormality of strong electrolytes,” *Physico-Chemical Laboratory, University College, Calcutta*, 1 1919.
- [16] D. S. P. Berg, “File:Na+H2O.svg - Wikimedia Commons,” 2006. [Online]. Available: <https://commons.wikimedia.org/wiki/File:Na%2BH2O.svg>
- [17] A. Dukhin, S. Parila, and P. Somasundaran, “Ion-Pair Conductivity Theory V: Critical Ion Size and Range of Ion-Pair Existence,” *Journal of the Electrochemical Society*, vol. 164, no. 14, 2018. [Online]. Available: <https://iopscience.iop.org/article/10.1149/2.0821814jes/meta>
- [18] R. Mancinelli, A. Botti, F. Bruni, M. A. Ricci, and A. K. Soper, “Hydration of Sodium, Potassium, and Chloride Ions in Solution and the Concept of Structure Maker/Breaker,” *J. Phys. Chem. B*, vol. 111, pp. 13 570–13 577, 2007. [Online]. Available: <https://pubs.acs.org/doi/10.1021/jp075913v>
- [19] L. Degrève, S. M. Vecchi, and C. Quintale Jr., “The hydration structure of the Na<sup>+</sup> and K<sup>+</sup> ions and the selectivity of their ionic channels,” *Biochimica et Biophysica Acta*, vol. 1274, pp. 149–156, 1996. [Online]. Available: <https://www.sciencedirect.com/science/article/pii/0005272896000199>
- [20] C. S. Widodo, H. Sela, and D. R. Santosa, “The effect of NaCl concentration on the ionic NaCl solutions electrical impedance value using electrochemical impedance spectroscopy methods,” *AIP Conference Proceedings*, 2018.
- [21] J. Vila, E. Rilo, L. Segade, O. Cabeza, and L. M. Varela, “Electrical conductivity of aqueous solutions of aluminum salts,” *Physical Review* 71, 2007.
- [22] E. Vitz, J. W. Moore, J. Shorb, X. Prat-Resina, T. Wendorff, and A. Hahn, “5.10: Coulomb’s Law - Chemistry LibreTexts,” 2020. [Online]. Available: [https://chem.libretexts.org/Bookshelves/General\\_Chemistry/Book%](https://chem.libretexts.org/Bookshelves/General_Chemistry/Book%205)
-

- [23] K. Malley and A. Singh, “Ionic Activity,” 2023.
- [24] Y. Avni, R. M. Adar, D. Andelman, and H. Orland, “Conductivity of Concentrated Electrolytes,” *Physical Review Letters*, vol. 128, 2022. [Online]. Available: <https://journals.aps.org/prl/pdf/10.1103/PhysRevLett.128.098002>
- [25] Y.-F. Hu, X.-M. Zhang, J.-G. Li, and Q.-Q. Liang, “Semi-ideal Solution Theory. 2. Extension to Conductivity of Mixed Electrolyte Solutions,” *The Journal of Physical Chemistry B*, vol. 112, no. 48, pp. 15 376–15 381, 12 2008.
- [26] A. Anderko and M. M. Lencka, “Computation of Electrical Conductivity of Multicomponent Aqueous Systems in Wide Concentration and Temperature Ranges,” *Industrial & Engineering Chemistry Research*, vol. 36, no. 5, pp. 1932–1943, 5 1997.
- [27] Y. M. Artemkina, V. V. Shcherbakov, and I. A. Akimova, “The Temperature Dependence of the Electrical Conductivity Activation Energy of the of Aqueous Electrolyte Solutions,” *Trans Tech Publications Ltd, Switzerland*, vol. 1031, pp. 228–233, 2021. [Online]. Available: <https://www.scientific.net/MSF.1031.228.pdf>
- [28] R. A. Horne and R. A. Courant, “The Temperature Dependence of the Activation Energy of the Electrical Conductivity of Sea Water in the Temperature Range 0C to 10C,” *Journal of Gephysical Research*, vol. 69, pp. 1152–1155, 1964. [Online]. Available: <https://agupubs.onlinelibrary.wiley.com/doi/pdfdirect/10.1029/JZ069i006p01152>
- [29] Y. Sato, “Physical Properties of High Temperature Molten Salts,” 2010.
- [30] “Cohesive and Adhesive Forces - Chemistry LibreTexts.” [Online]. Available: [https://chem.libretexts.org/Bookshelves/Physical\\_and\\_Theoretical\\_Chemistry\\_Textbook\\_Maps/Supplemental\\_Modules\\_\(Physical\\_and\\_Theoretical\\_Chemistry\)/Physical\\_Properties\\_of\\_Matter/States\\_of\\_Matter/Properties\\_of\\_Liquids/Cohesive\\_and\\_Adhesive\\_Forces](https://chem.libretexts.org/Bookshelves/Physical_and_Theoretical_Chemistry_Textbook_Maps/Supplemental_Modules_(Physical_and_Theoretical_Chemistry)/Physical_Properties_of_Matter/States_of_Matter/Properties_of_Liquids/Cohesive_and_Adhesive_Forces)
- [31] M. M. Walz and D. van der Spoel, “Microscopic origins of conductivity in molten salts unraveled by computer simulations,” *Communications Chemistry 2021 4:1*, vol. 4, no. 1, pp. 1–10, 1 2021. [Online]. Available: <https://www.nature.com/articles/s42004-020-00446-2>

- 
- [32] S. Takatsuka and M. Oshitani, "PRIMARY BATTERIES – RESERVE SYSTEMS — Thermally Activated Batteries: Overview," *Encyclopedia of Electrochemical Power Sources*, pp. 129–136, 2009.
- [33] A. Redkin, Y. Zaikov, O. Tkatcheva, and A. Shuryghin, "A Physical Model of Molten Salt Data," *Zeitschrift für Naturforschung A*, vol. 63, no. 7-8, pp. 462–466, 2008.
- [34] E. Van Artsdalen and I. S. Yaffe, "ELECTRICAL CONDUCTANCE AND DENSITY OF MOLTEN SALT SYSTEMS: KCl-LiCl, KCl-NaCl AND KCl-KI," Chemistry Division, Oak Ridge National Laboratory, Oak Ridge, Tennessee, Tech. Rep., 10 1954.
- [35] J. Clark, "Chlorides of Period 3 Elements."
- [36] C. R. BOSTON, "Densities of Molten AlCl<sub>3</sub> and NaCl-AlCl<sub>3</sub> Mixtures," Metals and Ceramics Division, Oak Ridge National Laboratory, Oak Ridge, Tennessee, Tech. Rep., 4 1966.
- [37] K. Mohandas, "An electrochemical investigation of the thermodynamic properties of the NaCl-AlCl<sub>3</sub> system at subliquidus temperatures," 2021.
- [38] Kannan and Desikan, "A CRITICAL APPRAISAL AND REVIEW OF ALUMINIUM CHLORIDE ELECTROLYSIS FOR THE PRODUCTION OF ALUMINIUM," Central Electrochemical Research Institute, Karaikudi, Tech. Rep., 1985.
- [39] H. Bloom and E. Heymann, "The electric conductivity and the activation energy of ionic migration of molten salts and their mixtures," Chemistry Department, University of Melbourne, Melbourne, Australia, Tech. Rep., 3 1946.
- [40] G. J. Janz, "Physical Properties and Structure of Molten Salts," *Journal of Chemical Education*, vol. 39, pp. 59–68, 1962. [Online]. Available: <https://pubs.acs.org/doi/pdf/10.1021/ed039p59>
- [41] A. Solheim, E. Skybakmoen, and B. Øye, "Carbochlorination routes in production of Al," 2 2018.
- [42] K. Grjotheim, C. Krohn, M. Malinovsky, K. Matiasovsky, and J. Thonstad, *Aluminium Electrolysis*, 2nd ed. Dusseldorf: Aluminium-Verlag, 1982.
- [43] T. Ishikawa and H. Ichikawa, "PROCESS FOR ELECTROLYTICALLY PRODUCING ALUMNUM," 1 1979.

- 
- [44] K. W. Morse and R. L. Rasmussen, "Aluminium Chloride," *ScienceDirect*, 2017.
- [45] ScienceDirect, "Eutectic Mixture," *Physical Metallurgy (Fourth Edition)*, 1996.
- [46] B. Kirchebner, M. Ploetz, C. Rehekampff, P. Lechner, and W. Volk, "Influence of Salt Support Structures on Material Jetted Aluminum Parts," *MDPI*, p. 3, 9 2021.
- [47] A. Abbasalizadeh and Y. Yongxiang, "Molten Salt Electrolytes," *ScienceDirect*, 2016.
- [48] Arthur D. Little, "A survey of potential processes for the manufacture of aluminium," Ph.D. dissertation, 1979.
- [49] ScienceDirect, "Cell Voltage - an overview — ScienceDirect Topics." [Online]. Available: <https://www.sciencedirect.com/topics/engineering/cell-voltage>
- [50] H. Nagamoto, "Fuel Cells: Electrochemical Reactions," *Encyclopedia of Materials: Science and Technology*, pp. 3359–3367, 1 2001.
- [51] E. P. Randviir and C. E. Banks, "Electrochemical impedance spectroscopy: an overview of bioanalytical applications," *Analytical Methods*, vol. 5, no. 5, p. 1098, 2013. [Online]. Available: [https://www.researchgate.net/publication/235982768\\_Electrochemical\\_impedance\\_spectroscopy\\_An\\_overview\\_of\\_bioanalytical\\_applications](https://www.researchgate.net/publication/235982768_Electrochemical_impedance_spectroscopy_An_overview_of_bioanalytical_applications)
- [52] E. Barsoukov and J. R. Macdonald, *Impedance Spectroscopy: Theory, Experiment, and Applications*, 2nd ed. Wiley, 2005.
- [53] "File:Complex Impedance.svg - Wikimedia Commons." [Online]. Available: [https://commons.wikimedia.org/wiki/File:Complex\\_Impedance.svg](https://commons.wikimedia.org/wiki/File:Complex_Impedance.svg)
- [54] Xinming Qian, Ningyu Gu, Zhiliang Cheng, Xiurong Yang, Erkang Wang, and Shaojun Dong, "Methods to study the ionic conductivity of polymeric electrolytes using a.c. impedance spectroscopy ," 2005.
- [55] H. S. Magar, R. Y. Hassan, and A. Mulchandani, "Electrochemical Impedance Spectroscopy (EIS): Principles, Construction, and Biosensing Applications," *Sensors (Basel, Switzerland)*, vol. 21, no. 19, 10 2021. [Online]. Available: [/pmc/articles/PMC8512860//pmc/articles/PMC8512860/?report=abstracthttps://www.ncbi.nlm.nih.gov/pmc/articles/PMC8512860/](https://pubmed.ncbi.nlm.nih.gov/pmc/articles/PMC8512860/)
- [56] J. e. Hammond, "Electrochemical biosensors and nanobiosensors," *Essays in Biochemistry*, vol. 60, pp. 69–80, 2016.
-

- 
- [57] K. Acord, “Electrochemical Impedance Spectroscopy ,” 2021. [Online]. Available: [https://eng.libretexts.org/Bookshelves/Materials\\_Science/Supplemental\\_Modules\\_\(Materials\\_Science\)/Insulators/Electrochemical\\_Impedance\\_Spectroscopy](https://eng.libretexts.org/Bookshelves/Materials_Science/Supplemental_Modules_(Materials_Science)/Insulators/Electrochemical_Impedance_Spectroscopy)
- [58] Heraeus, “Properties of Fused Silica.” [Online]. Available: [https://www.heraeus.com/en/hca/fused\\_silica\\_quartz\\_knowledge\\_base\\_1/properties\\_1/properties\\_hca.html#tabs-608478-5](https://www.heraeus.com/en/hca/fused_silica_quartz_knowledge_base_1/properties_1/properties_hca.html#tabs-608478-5)
- [59] “Sublimation Point - an overview — ScienceDirect Topics.” [Online]. Available: <https://www.sciencedirect.com/topics/chemistry/sublimation-point>
- [60] J. Barthel, R. Buchner, and M. Münsterer, *Electrolyte Data Composition - Part 2: Dielectric Properties of Water and Aqueous Electrolyte Solutions*, 2nd ed., G. Kreysa, Ed. Regensburg: DECHEMA, 1995, vol. XII.
- [61] D. R. Liu, W. X. Li, Z. H. Yang, S. L. Qiu, and Y. T. Luo, “Electrochemical investigation on kinetics of potassium intercalating into graphite in KF melt,” *Transactions of Nonferrous Metals Society of China*, vol. 21, no. 1, pp. 166–172, 1 2011.
- [62] K. H. Stern, “Glass-Molten Salt Interactions,” *Chemical Reviews*, vol. 66, no. 4, pp. 355–371, 1966.
- [63] “4.3: Resistance and Temperature - Physics LibreTexts.” [Online]. Available: [https://phys.libretexts.org/Bookshelves/Electricity\\_and\\_Magnetism/Electricity\\_and\\_Magnetism\\_\(Tatum\)/04%3A\\_Batteries\\_Resistors\\_and\\_Ohm's\\_Law/4.03%3A\\_Resistance\\_and\\_Temperature](https://phys.libretexts.org/Bookshelves/Electricity_and_Magnetism/Electricity_and_Magnetism_(Tatum)/04%3A_Batteries_Resistors_and_Ohm's_Law/4.03%3A_Resistance_and_Temperature)
- [64] E. M. Levin, J. F. Kinney, R. D. Wells, and J. T. Benedict, “The System NaCl-AICI 3,” *JOURNAL Of RESEARCH of the National Bureau of Standards-A. Physics and Chemistry*, vol. 78, no. 4.
- [65] Janz et.al., “Electrical Conductance, Density, Viscosity, and Surface Tension Data,” *Molten Salts*, vol. 4, pp. 1062–1063, 1975.
- [66] National Library of Medicine National, “Aluminum Chloride.”

---

---

---

## Appendices

---

---



# A Varying concentrations in aqueous solutions

The average measured resistances presented in Table 4.1 and 4.3 are all calculated from three separate measurements. All measurements are presented in Table A.1 and A.2.

**Table A.1:** Resistance [ $\Omega$ ] for various salt solutions.

Measurement	1 M NaCl	2 M NaCl	Saturated NaCl	1 M KCl	2 M KCl
<b>1</b>	541.789	311.943	184.285	417.026	225.702
<b>2</b>	546.047	311.346	185.653	416.870	227.154
<b>3</b>	538.447	312.514	185.779	416.932	227.773

**Table A.2:** Resistance [ $\Omega$ ] measurements for various mixing ratios of salt solutions.

Measurement	50-50	60-40 KCl-NaCl	40-60 KCl-NaCl	20-80 KCl-NaCl	80-20 KCl-NaCl
<b>1</b>	468.234	458.923	477.645	506.844	430.409
<b>2</b>	469.226	464.709	480.143	511.690	431.185
<b>3</b>	469.528	464.639	481.476	511.232	432.040

The cell constant used in calculations for all experiments in aqueous solutions where calculated from measured resistance and tabular conductivity of various concentrations and compositions of NaCl and KCl presented in Table 4.1 and 4.3. A cell constant for each sample was calculated, and an average cell constant was then used in further measurements. The cell constants calculated from tabular conductivity values are presented in Table A.3.

---

**Table A.3:** Calculated cell constant for various salt solutions.

Salt solution	Calculated cell constant [ $\text{cm}^{-1}$ ]
1 M NaCl	46.089
2 M NaCl	45.134
1 M KCl	45.314
2 M KCl	45.203
60-40 KCl-NaCl	45.730
40-60 KCl-NaCl	45.025
20-80 KCl-NaCl	45.414
80-20 KCl-NaCl	44.760

The average cell constant was calculated to  $45.333 \text{ cm}^{-1}$ . This is the cell constant used in further calculations. The average standard deviation for the average cell constant was determined to be  $(\pm) 0.147 \text{ cm}^{-1}$ . The equations used to find this deviation are presented in Appendix F.

From the measured resistances and calculated cell constant, the conductivity of the solutions was calculated from Equation 2.3. A calculation example using 1 M NaCl at  $25 \text{ }^\circ\text{C}$  is shown below:

$$\kappa(1MNaCl) = \frac{1}{542.094\Omega} \times 45.222\text{cm}^{-1} = 0.084 \frac{S}{\text{cm}} \quad (\text{A.1})$$

The calculation of the expected conductivity of aqueous solutions with varying composition NaCl (1 M) and KCl (1 M) was calculated from their calculated conductivity. An example showing the calculation 80-20 KCl-NaCl shown below:

$$\kappa(80-20KCl-NaCl) = (0.8 \times 0.1087 \frac{S}{\text{cm}}) + (0.2 \times 0.0836 \frac{S}{\text{cm}}) = 0.1037 \frac{S}{\text{cm}} \quad (\text{A.2})$$

This calculation assumes that there is no introduction of additional interactions between the species of the two salts.

## B Cell constant quartz cell

The resistance measurements of various salt solutions in the first quartz cell are presented in Table B.1:

**Table B.1:** Resistance [ $\Omega$ ] measurements for various salt solutions in quartz cell 1.

Measurement	1 M NaCl	2 M NaCl	1 M KCl	2 M KCl
1	510.140	290.127	390.597	208.818
2	509.646	287.643	391.144	208.789
3	509.458	287.523	389.693	208.774

From the measurements in Table B.1, the average measured resistance of each sample was used to find the cell constant from tabular conductivity. The cell constants are shown in Table B.2:

**Table B.2:** Calculated cell constant for various salt solutions measured in quartz cell 1.

Salt solution	Calculated cell constant [ $\text{cm}^{-1}$ ] in quartz cell 1
1 M NaCl	43.339
2 M NaCl	41.746
1 M KCl	42.352
2 M KCl	41.596

From Table B.2, the average cell constant of the first quartz cell was determined to be  $42.258 \text{ cm}^{-1}$ .

The resistance measurements of various salt solutions in the second quartz cell are presented in Table B.3:

---

**Table B.3:** Resistance [ $\Omega$ ] measurements for various salt solutions in quartz cell 2.

Measurement	1 M NaCl	2 M NaCl	1 M KCl	2 M KCl
1	472.476	276.414	362.930	195.431
2	472.456	276.387	363.747	195.495
3	473.907	276.634	364.449	195.443

From the measurements in Table B.3, the average measured resistance of each sample was used to find the cell constant from tabular conductivity. The cell constants are shown in Table B.4:

**Table B.4:** Calculated cell constant calculations for various salt solutions measured in quartz cell 2.

Salt solution	Calculated cell constant [ $\text{cm}^{-1}$ ] in quartz cell 2
1 M NaCl	40.210
2 M NaCl	40.004
1 M KCl	39.528
2 M KCl	38.943

From Table B.4, the average cell constant of the second quartz cell was determined to be  $39.671 \text{ cm}^{-1}$ .

## C Calculation of salt compositions in high temperature experiments

The densities of the molten salts mixtures were used to calculate the required mass to get a total volume of 7 mL molten salt in the quartz cell. The tabular density for the lowest measured temperature and a mean molar mass of the components were used for the calculations. As an example, the calculation of mass NaCl and KCl required in a 50-50 mol% composition is shown below.

The density of a 50-50 mol% NaCl-KCl melt at 690°C equals  $1.588 \frac{g}{cm^3}$ , and was used to calculate the total mass salt needed to achieve a total volume of 7 mL when molten. All densities used in calculations are found in [65].

$$m_{total} = 7cm^3 \times 1.588 \frac{g}{cm^3} = 11.116g \quad (C.1)$$

The mean molar mass was calculated from the components in the mixture:

$$Mm_{mean} = \frac{(58.44 + 74.55) \frac{g}{mol}}{2} = 66.50 \frac{g}{mol} \quad (C.2)$$

From the mean molar mass, the required mass of each component was calculated:

$$n_{total} = \frac{mass_{total}}{Mm_{mean}} = 0.167mol \quad (C.3)$$

$$n_{NaCl} = n_{KCl} = 50\% \times n_{total} = 0.084mol \quad (C.4)$$

$$m_{NaCl} = 0.084mol \times 58.44 \frac{g}{mol} = 4.88g \quad (C.5)$$

$$m_{KCl} = 0.084mol \times 74.55 \frac{g}{mol} = 6.23g \quad (C.6)$$

## D Weighed quantity of salt for experiments with hygroscopic molten salts

The mass of NaCl, KCl, and AlCl<sub>3</sub> used in the experiments containing AlCl<sub>3</sub> are presented in Table D.1. The average molar mass is 88.777, which can be used to calculate the total number of mols, determined to be 0.150 mol. The mol percentages used for NaCl, KCl, and AlCl<sub>3</sub> are 48.5 %, 48.5 %, and 3 %, respectively.

**Table D.1:** Total mass weighed out for the mixture with eutectic composition of NaCl-KCl + 3 mol% of AlCl<sub>3</sub>.

	NaCl	KCl	AlCl <sub>3</sub>
Molar mass	58.44	74.55	133.34
Mole component	0.073	0.073	0.005
<b>Mass component</b>	<b>4.263</b>	<b>5.439</b>	<b>0.602</b>

The following table shows how the required mol of AlCl<sub>3</sub> was found from NaAlCl<sub>4</sub> and the associated mass used:

**Table D.2:** Mass from the eutectic composition of NaCl-AlCl<sub>3</sub>.

Molar ratio NaCl-AlCl <sub>3</sub>	1-1
Molar mass NaAlCl <sub>4</sub>	191.783 g
Mol% AlCl <sub>3</sub> required	3%
Mass total NaAlCl <sub>4</sub>	0.865 g
Mass NaCl	0.264 g
Mass AlCl <sub>3</sub>	0.602 g

Based on the information presented in Tables D.1 and D.2, it can be determined that an additional 3.999 g of NaCl is required to reach a total mass of 4.263 g. For the sake of simplicity, it was decided to maintain identical weighing and composition to that of the first experiment while adding 1 g of LiCl. This addition of 1 g LiCl resulted in a molar fraction of 15.683 % for LiCl in the composition.

# E Finding average measured resistance from Nyquist plots

An example of finding the resistance of an aqueous salt solution (80-20 KCl-NaCl) with following Nyquist plots is shown below. The tables containing the exact coordinates of the points shown in the Nyquist plots are also presented. The  $Z_{\text{real}}$  value used in further calculations and its corresponding  $Z_{\text{imag}}$  is highlighted. From the selected values of the three separate measurements presented, an average measured resistance was calculated and used in further calculations.

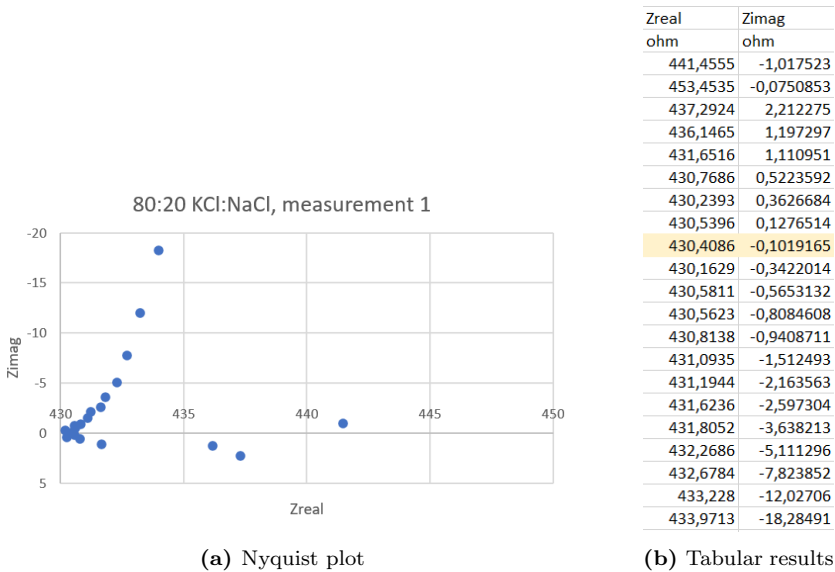
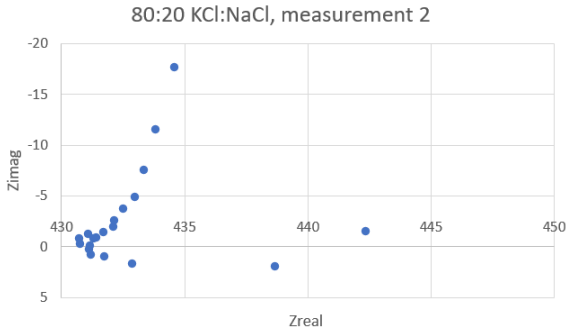


**Figure E.1:** Experimental results for impedance measurements of 80-20 mol% KCl-NaCl presented in both Nyquist plot and table, first measurement.

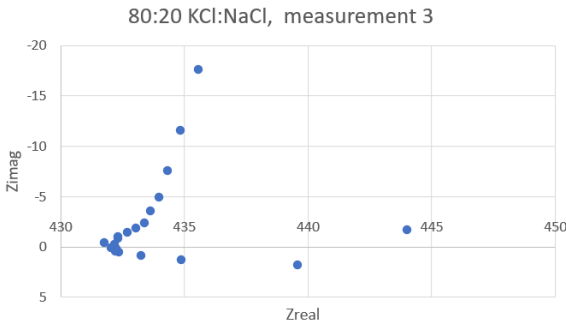


(a) Nyquist plot

Zreal	Zimag
ohm	ohm
442,3935	-1,480819
454,8952	-0,11308
438,6969	2,046179
432,9098	1,699402
431,7868	1,045164
431,2106	0,8794049
431,1356	0,2840222
430,7668	-0,198248
431,1845	-0,002063
430,7525	-0,70735
431,117	-1,219975
431,4363	-0,84412
431,3248	-0,753658
431,7245	-1,325746
432,1226	-1,858138
432,1663	-2,515767
432,5507	-3,677337
433,0065	-4,843253
433,3547	-7,487459
433,8635	-11,51014
434,6008	-17,56219

(b) Tabular results

**Figure E.2:** Experimental results for impedance measurements of 80-20 mol% KCl-NaCl presented in both Nyquist plot and table, second measurement.



(a) Nyquist plot

Zreal	Zimag
ohm	ohm
444,0203	-1,679244
455,4147	-0,0256435
439,5746	1,862127
434,8791	1,340265
433,2727	0,9214187
432,3765	0,5139896
432,0399	0,158435
432,2558	0,2268279
432,2037	-0,2576329
432,2393	0,4492612
431,7687	-0,4161113
432,321	-0,7944099
432,3347	-1,008172
432,7179	-1,404132
433,0421	-1,818715
433,3981	-2,354743
433,6269	-3,49895
433,9896	-4,898005
434,3452	-7,517362
434,8403	-11,53681
435,561	-17,60336

(b) Tabular results

**Figure E.3:** Experimental results for impedance measurements of 80-20 mol% KCl-NaCl presented in both Nyquist plot and table, third measurement.



## F Calculations of standard and percentage deviations

The standard deviation of resistance measured in aqueous solutions is calculated from Equation F.1

$$s = \sqrt{\frac{\sum(x_i - \bar{x})^2}{N - 1}} \quad (\text{F.1})$$

In Equation F.1, the 3 measurements done at the relevant sample were used. The standard deviation for the average measured resistance was calculated from Equation F.2. This is the standard deviation presented in the results.

$$\bar{s} = \frac{s}{\sqrt{N}} \quad (\text{F.2})$$

The percentage standard deviation was found from Equation F.3:

$$\%deviation = \frac{\bar{s}_R}{R} \times 100\% \quad (\text{F.3})$$

From the resistance's standard deviation, the percentage deviation of the conductivity was found from Equation F.4:

$$s_\kappa = \sqrt{\left(\frac{\bar{s}_R}{R}\right)^2} \quad (\text{F.4})$$

Percentage deviations for the conductivity was calculated as shown in Equation F.3. When calculating standard and percentage deviation of resistance and conductivity in molten salts, the same equations were applied.

## G Impedance measurements at varying temperatures for aqueous solutions

The resistance measurements used to calculate the conductivities of NaCl (1 M) and KCl (1 M) shown in Figure 4.3 are shown below in Table G.1 and G.2.

**Table G.1:** Measurement data for NaCl at different temperatures.

Measurement [ $\Omega$ ]	30 °C	40 °C	50 °C
1	486.9536	408.2457	348.9332
2	486.0552	408.2275	349.0224
3	486.3508	408.0388	349.0531

**Table G.2:** Measurement data for KCl at different temperatures.

Measurement [ $\Omega$ ]	30 °C	40 °C	50 °C
1	378.3194	322.4911	282.6533
2	378.7252	322.1022	282.2243
3	378.483	321.4355	282.0152

Table G.3 and G.4 displays the data used to obtain the plots in Figure 4.3 and 4.4.

**Table G.3:** Resistance measurements, calculated conductivity and tabular conductivity for KCl (1 M) at 30 °C, 40 °C and 50 °C.

Temperature	Average measured resistance [ $\Omega$ ]	Standard deviation resistance [ $\Omega$ ]	Calculated conductivity [S/cm]	Tabular conductivity values [S/cm]
30°C	378.509	0.204	0.120	0.118
40°C	322.010	0.534	0.141	0.138
50°C	282.298	0.325	0.161	0.158

---

**Table G.4:** Resistance measurements and calculated conductivity for NaCl (1 M) at 30 °C, 40 °C and 50 °C.

<b>Temperature</b>	<b>Average measured resistance [<math>\Omega</math>]</b>	<b>Standard deviation resistance [<math>\Omega</math>]</b>	<b>Calculated conductivity [S/cm]</b>
<b>30°C</b>	486.453	0.458	0.093
<b>40°C</b>	408.171	0.115	0.111
<b>50°C</b>	349.003	0.062	0.129

## H All measurements molten salts

All the resistances measured for the molten salt systems are presented in the tables below.

**Table H.1:** Measurement data for eutectic composition of NaCl-KCl at different temperatures.

Measurement [ $\Omega$ ]	700 °C	750 °C	800 °C
<b>1</b>	18.745	17.738	16.918
<b>2</b>	18.745	17.709	16.896
<b>3</b>	18.760	17.706	16.911

**Table H.2:** Measurement data for 80-20 mol% NaCl-KCl at different temperatures.

Measurement [ $\Omega$ ]	730 °C	750 °C	770 °C	800 °C
<b>1</b>	15.310	15.027	14.770	14.444
<b>2</b>	15.305	15.020	14.778	14.438
<b>3</b>	15.310	15.017	14.773	14.437

**Table H.3:** Measurement data for eutectic NaCl-KCl composition added 20 mol% LiCl at different temperatures.

Measurement [ $\Omega$ ]	700 °C	730 °C	750 °C	770 °C	800 °C
<b>1</b>	17.300	16.752	16.384	16.096	15.663
<b>2</b>	17.282	16.751	16.391	16.087	15.682
<b>3</b>	17.320	16.737	16.398	16.088	15.632

---

**Table H.4:** Measurement data for eutectic NaCl-KCl composition added 3 mol% AlCl<sub>3</sub> at different temperatures.

Measurement [ $\Omega$ ]	700 °C	730 °C	750 °C	770 °C	800 °C
<b>1</b>	20.043	19.162	18.763	18.340	17.762
<b>2</b>	19.944	19.188	18.728	18.316	17.732
<b>3</b>	19.975	19.201	18.705	18.293	17.742

**Table H.5:** Measurement data for eutectic NaCl-KCl composition added 3 mol% AlCl<sub>3</sub> and 1 g LiCl at different temperatures.

Measurement [ $\Omega$ ]	700 °C	730 °C	750 °C	770 °C	800 °C
<b>1</b>	19.077	18.360	17.954	17.553	17.030
<b>2</b>	19.041	18.342	17.947	17.534	17.095
<b>3</b>	19.013	18.346	17.925	17.548	17.052

# I HSE data

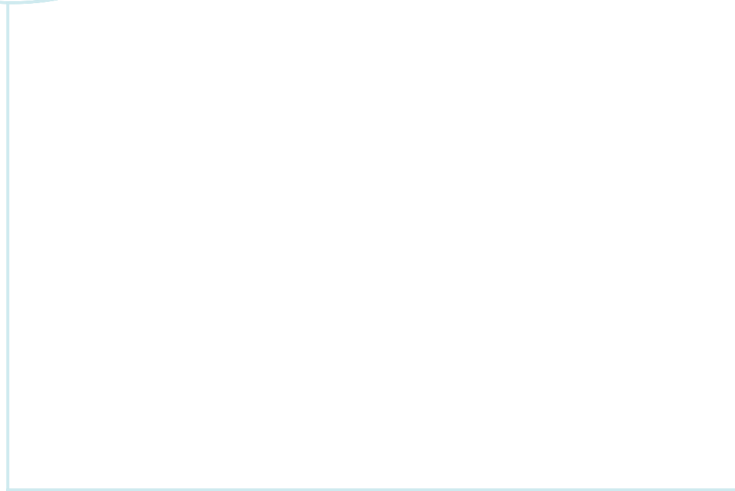
The H/P phrases of  $\text{AlCl}_3$  and  $\text{LiCl}$  are presented in Figure I.1 and I.2.

<p><b>Signal Word</b></p> <p>Danger</p> <p><b>Hazard Statements</b></p> <p>H314 - Causes severe skin burns and eye damage</p> <p><b>EU Specific Hazard Statements</b></p> <p>EUH014 - Reacts violently with water</p> <p><b>Precautionary Statements</b></p> <p>P280 - Wear protective gloves/protective clothing/eye protection/face protection</p> <p>P301 + P330 + P331 - IF SWALLOWED: Rinse mouth. Do NOT induce vomiting</p> <p>P303 + P361 + P353 - IF ON SKIN (or hair): Take off immediately all contaminated clothing. Rinse skin with water or shower</p> <p>P305 + P351 + P338 - IF IN EYES: Rinse cautiously with water for several minutes. Remove contact lenses, if present and easy to do. Continue rinsing</p> <p>P310 - Immediately call a POISON CENTER or doctor/physician</p>
---

**Figure I.1:** H/P phrases for  $\text{AlCl}_3$ .

<p><b>Signal Word</b></p> <p>Warning</p> <p><b>Hazard Statements</b></p> <p>H302 - Harmful if swallowed</p> <p>H315 - Causes skin irritation</p> <p>H319 - Causes serious eye irritation</p> <p><b>Precautionary Statements</b></p> <p>P301 + P312 - IF SWALLOWED: Call a POISON CENTER or doctor/physician if you feel unwell</p> <p>P305 + P351 + P338 - IF IN EYES: Rinse cautiously with water for several minutes. Remove contact lenses, if present and easy to do. Continue rinsing</p> <p>P280 - Wear protective gloves/protective clothing/eye protection/face protection</p> <p>P302 + P352 - IF ON SKIN: Wash with plenty of soap and water</p>
--

**Figure I.2:** H/P phrases for  $\text{LiCl}$ .



 **NTNU**

Norwegian University of  
Science and Technology